expression of the entire transcript was confirmed during Caco-2 cell differentiation (Fig. 4C). Therefore, we examined the genomic structure of pri-miR-194-2 that gives rise to a part of the inducible miR-194 during intestinal epithelial cell differentiation.

Identification of the core promoter element for pri-miR-194-2

To know the transcriptional mechanism, we then sought to analyze the promoter region of pri-miR-194-2. Upstream genomic region close to the transcription start site of pri-miR-194-2 contains several highly conserved regions among human, mouse, rat, and dog (from −162 to +21 with respect to the transcription start site of AK092802) (Fig. 5A). To identify the promoter region, we constructed reporter plasmids carrying various genomic sequences around the transcription start site of pri-miR-194-2 (Fig. 5B) and subjected them to luciferase assay. Results demonstrated that the region from −162 to +21 had a high promoter activity in differentiated Caco-2 cells, comparable to that of the longest region from −1003 to +358 (Fig. 5B). In contrast, deletion of the conserved region dramatically reduced promoter activity.

Since conserved regions in a gene promoter are expected to contain regulatory elements, we focused on such region found within the pri-miR-194-2 promoter. Luciferase assay using a mutated construct revealed that the region from −70 to −52 is critically required for the pri-miR-194-2 promoter activity that is driven by the identified conserved region in differentiated Caco-2 cells, indicating that the corresponding region is the core element of pri-miR-194-2 promoter (Fig. 5C).

HNF-1α regulates pri-miR-194-2 promoter

By a computational search for potential motifs of transcription factors, a putative binding site for HNF-1α was found in the conserved core element of pri-miR-194-2 promoter (Fig. 6A). HNF-1α is a member of a class of transcription factors that is distantly related to homeobox proteins, which contains a DNA binding domain. In addition, HNF-1α has been formerly described as a key transcriptional activator during Caco-2 differentiation (Wu et al. 1994; Mitchelmore et al. 1998; Boudreau et al. 2001, 2002; van Wering et al. 2002). Thus, we hypothesized that HNF-1α might bind to the core element of pri-miR-194-2 promoter and contribute to upregulate pri-miR-194-2 transcription. Indeed, HNF-1α was shown to physically interact to the core element of the pri-miR-194-2 promoter in Caco-2 cells, as judged by ChIP assay (Fig. 6B). Furthermore, forced expression of HNF-1α activated the promoter of both pri-miR-194-2 and SI in HeLa S3 cells, which usually do not express miR-194 (Fig. 6C). Forced expression of HNF-1α in Caco-2 cells also showed an additive effect on the promoter activity of pri-miR-194-2. Mutation in the HNF-1α binding site resulted

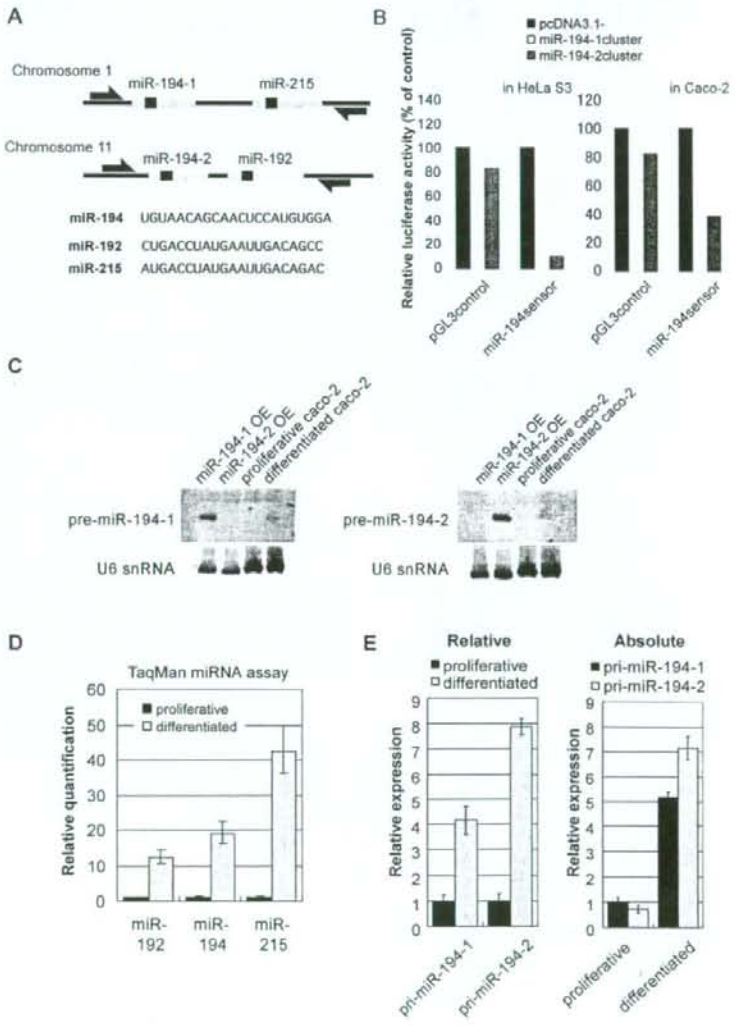

FIGURE 2. (Legend on next page)

in almost complete loss of the pri-miR-194-2 promoter activity, confirming the requirement of HNF-1α binding to the corresponding site for pri-miR-194-2 transcription. Taken together, these data suggest that HNF-1α is a key transcriptional regulator of pri-miR-194-2 and activates its promoter activity by physically binding to the core promoter element.

DISCUSSION

In the present study, we identified the structure of pri-miR-194-2 and determined both transcription start site and 3′ end using 5′ RACE and 3′ RACE, respectively. As pri-miRNAs could be either a protein-coding RNA or a noncoding RNA, we searched in silico for a candidate open reading frame (ORF) within a pri-miR-194-2, -192 transcript and did not find a single protein-coding ORF. In addition, conserved genomic region of pri-miR-194-2, -192 was restricted to the region encoding miRNA hairpin structures. Therefore, we suggest that pri-miR-194-2, -192 is a noncoding RNA.

We also identified that miR-194-2 and miR-192 are encoded within the intron but not in the exon (Fig. 4B). To assure this, we have shown that mature miR-194 surely arises from the miR-194-2, -192 cluster region, a partial sequence of the second intron (Fig. 4B), by forced expression of the corresponding region (Fig. 2B). This means that these miRNAs are processed by splicing and cropping of the pri-miRNA in the nucleus. Indeed, although the PCR product shown in Figure 3B contained the second intron, the PCR product shown in Figure 4C lacked the corresponding intron sequence. This difference may be attributed to the relatively short extension time (1.5 min) used for the PCR in Figure 4C, for detection of the transcript containing the intron (4.8 kb), but also suggests that the second intron containing the miR-194-2, -192 cluster is primarily transcripted along with the three exons but is rapidly spliced out from the pri-miR-194-2.

On the other hand, concerning these processing steps, a model of intronic miRNA processing was recently suggested (Kim and Kim 2007). According to their model, miRNA-harboring intron is detained while other introns are rapidly spliced out. In our study, RT-PCR analysis in Figure 3B showed 2.4-kbp and 1.8-kbp products, which might represent the nascent transcript and the partially spliced transcript for pri-miR-194-2, respectively. As the reverse primer used in the present RT-PCR is placed within the second intron, the result may indicate that the first intron is processed more rapidly, compared with the miRNA-harboring second intron. Therefore, pri-miR-194-2 might be processed through the proposed model.

Also in our study, we demonstrated that miR-194 is highly expressed in differentiated intestinal epithelial cells. Induced expression of miR-194 could be accounted by the regulatory mechanism of *miR-194-2* gene in that a tissue-associated transcription factor, HNF-1α, plays a central role in its transcription. Although HNF-1α is well known for its regulatory roles of various genes specific for the intestine, its expression is not tightly restricted to the intestine but is also found in the liver or the kidney (Mendel and Crabtree 1991). However, mature miR-194 has been reported to appear not only in the intestine but also in the liver and in the kidney (Lagos-Quintana et al. 2003; Krutzfeldt et al. 2005; Wienholds et al. 2005; Kato et al. 2007). Our TaqMan miRNA analyses have also confirmed expression of miR-194 in these tissues (Fig. 1F). These findings are consistent with our present study describing the regulation of miR-194 expression by HNF-1α. Recent studies, however, have highlighted the regulation of mature miRNA generation at the post-transcriptional processing level (Thomson et al. 2006; Viswanathan et al. 2008) Although our data show consistent increase of mature miR-194 upon increase of its pri-miRNAs, there remains a possibility that expression of mature miR-194 might also be regulated at the processing level.

Our promoter analyses revealed that the consensus motif for HNF-1α found within the conserved region of the pri-miR-194-2 promoter plays a critical role in induction of *miR-194-2* gene upon Caco-2 cell differentiation. HNF proteins are known to interact with other transcription factors to regulate the expression of various intestine-specific genes. For example, different members of the HNF family that are expressed in the intestine, such as HNF-1β and

FIGURE 2. Expression of miR-194-2, -192 cluster was induced during Caco-2 differentiation. (*A*) Genomic organization of miR-194 clusters. miR-194-1 and miR-215 are located within an ~400-bp region in chromosome 1. miR-194-2 and miR-192 are located within an ~300-bp region in chromosome 11. Open arrows represent pri-miRNA detection primers used in *E*. (*B*) Both miR-194 loci potentially express mature miR-194. miR-194 expression vector and pGL3miR-194sensor were cotransfected into HeLa S3 cells (*left*) or Caco-2 cells (*right*). As pGL3miR-194sensor contained a sequence completely complementary to mature miR-194 in 3′UTR of luciferase, expression of mature miR-194 is detected by reduced firefly luciferase activity by RNAi. Firefly luciferase reporter activities were normalized by *Renilla* luciferase. The mean value of cells cotransfected with pcDNA3.1 mock vector was set to 100. (*C*) Northern blot of the pre-miR-194s, each arising from distinct loci. Total RNA (30 μg) extracted from proliferative or differentiated Caco-2 cells that were pretreated with Dicer siRNA was analyzed. Positive control (10 μg total RNA) was obtained from Dicer knockdowned 293 cells transfected with miR-194 cluster expression vectors (miR-194-1 OE and miR-194-2, OE, respectively). Probes were designed to hybridize around the loop sequence of each transcript. (*D*) Inducible expression of miRNAs from miR-194 clusters during Caco-2 differentiation. Expression of miR-192, miR-194, and miR-215 were quantified by TaqMan miRNA assay. U6 snRNA was used as endogenous control to normalize expression of miRNAs. The expression level of each miRNA in proliferative Caco-2 cells was set to 1. (*E*) Two distinct miR-194 loci contribute to its induced expression during Caco-2 cell differentiation. RT-PCR was performed with primers indicated in *A*, and GAPDH was used as endogenous control. For relative quantification, expression of each pri-miR-194 within proliferative Caco-2 was used as a standard (*left*). For absolute quantification, genomic DNA was used as a standard. Bar graph is drawn so that pri-miR-194-1 in proliferative Caco-2 cells is set to 1 (*right*).

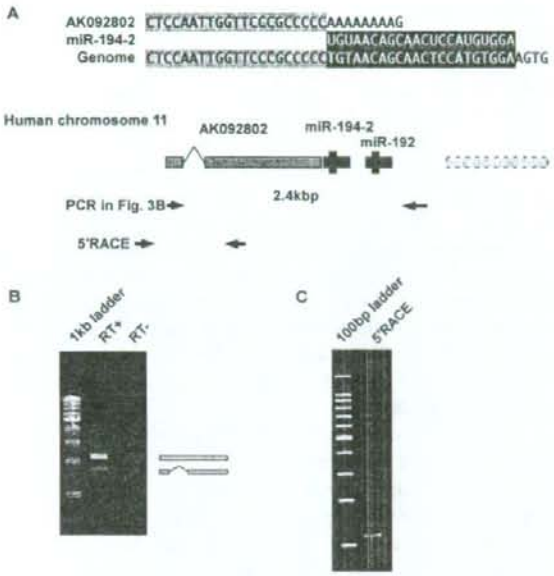

FIGURE 3. Identification of the transcription start site of pri-miR-194-2. (*A*) Genomic sequence and EST information surrounding miR-194-2. 3′ End of AK092802 is adjacent to 5′end of miR-194. Arrow bars represent predicted PCR products. (*B*) AK092802 and miR-194-2, -192 cluster are linked in a single transcript. RT-PCR was performed by total RNA extracted from differentiated Caco-2 cells, using primers indicated in *A*. PCR products were separated by 1% agarose gel electrophoresis and stained by EtBr. Sequence analysis of the amplified products revealed that the 2.4-kbp fragment contained an intronic sequence, while the intronic sequence was spliced out in the 1.8-kbp fragment. (*C*) 5′ RACE analysis of pri-miR-194-2. 5′ RACE was performed using random primers instead of oligo dT primer. PCR was performed by primers indicated in *A*. PCR products were separated by 5% polyacrylamide gel electrophoresis and stained by EtBr. Consistent with *B*, two fragments were observed, and sequence analysis of these fragments revealed that difference was due to an intronic sequence. Both fragments had the same transcription start site.

HNF-4, coordinately enhance target gene expression (Wu et al. 1994; Hu and Perlmutter 1999, 2002; Boudreau et al. 2001). Furthermore, GATA family and caudal related homeobox protein Cdx2 also coordinately enhance expression of intestine-specific genes (Krasinski et al. 2001; Boudreau et al. 2002; Wang et al. 2004). It is therefore speculated that the consensus motif for HNF-1α found within the core promoter region of pri-miR-194-2 may play a pivotal role in different aspects of regulation for this miRNA. Evolutional conservation of this consensus site among phylogenetically distant species further indicates a strong functional link between HNF-1α and miR-194-2 expression and also its significance in essential physiological events.

From the view of environmental regulation of miRNA, a recent study reported that miR-192 ectopically appears in diabetic renal glomeruli and that TGF-β is involved in the induction of this miRNA (Kato et al. 2007). As we have determined in the present study that miR-192 is the clustering partner of miR-194-2, it is possible that TGF-β may also regulate expression of miR-194. Interestingly, it is reported that TGF-β1 can modulate the differentiation process of Caco-2 cells in certain environments (Schroder et al. 1999). Therefore, it is of interest to examine the role of TGF-β upon regulation of miR-194 expression, as this cytokine shows diverse effects on intestinal physiology.

In conclusion, miR-194 is highly induced during intestinal epithelium differentiation, and pri-miR-194-2 expression

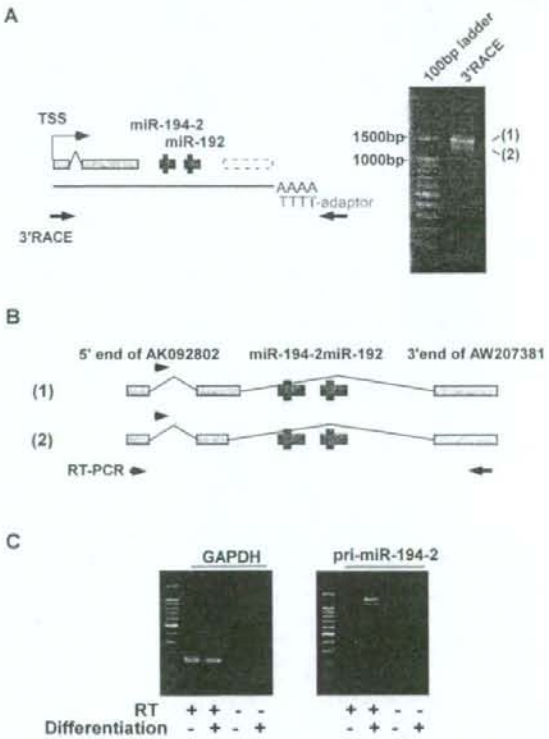

FIGURE 4. Identification of pri-miR-194-2 structure. (*A*) 3′ RACE analysis of pri-miR-194-2. Schematic representation of the primers used in the analysis is shown (*left*). PCR products were separated by 2% agarose gel electrophoresis and stained by EtBr (*right*). Two fragments are shown, designated as 1 and 2. (*B*) Schematic representation of pri-miR-194-2 structures. Sequence analysis revealed that difference in fragments 1 and 2 observed in *A* comes from the difference in length of the second exon. Both fragments had the same 3′ end, which also coincided with the 3′ end of AW207381. (*C*) Induced expression of pri-miR-194-2 during Caco-2 cell differentiation. To confirm the increased expression of the identified pri-miR-194-2 transcript during Caco-2 differentiation, RT-PCR was performed using primers represented in *B*. PCR products were separated by 2% agarose gel electrophoresis, and stained by EtBr.

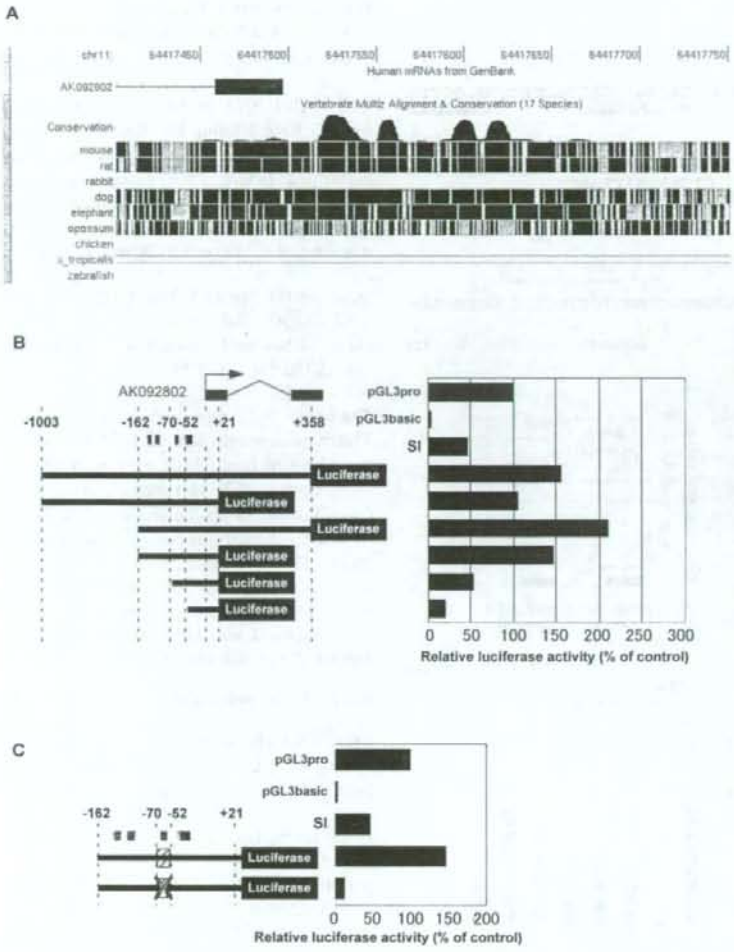

FIGURE 5. Potential HNF-1α binding element is located in the pri-miR-194-2 promoter. (*A*) Conserved sequences found within the pri-miR-194 promoter region. This figure is derived from the UCSC genome browser. (*B*) Schematic representation of human miR-194-2 promoter reporter constructs (*left*) and analysis of their promoter activity (*right*). Firefly luciferase reporter plasmids were constructed containing various regions of the putative pri-miR-194-2 promoter between positions −1003 to +358, designated with respect to the 5′end of AK092802. Arrow indicates transcription start site of pri-miR-194-2. pGL3 promoter (pGL3 pro) contains SV40 promoter, while pGL3basic has no promoter sequence upstream of the luciferase coding region. (*C*) Mutation of the region from −70 to −52 dramatically reduced pri-miR-194-2 promoter activity in Caco-2 cells. A scrambled sequence was introduced in the mutant pri-miR-194-2 promoter. Luciferase activities were normalized by *Renilla* luciferase activities.

is regulated by HNF-1α. As HNF-1α is one of the critical regulators of intestinal epithelial gene expression, control of miR-194 by this transcription factor adds miRNAs to the regulatory network of gene expression in intestinal epithelial cells. Therefore, the present work suggests that induced expression of miRNAs by tissue-specific transcription factors has an important role in intestinal epithelium maturation.

MATERIALS AND METHODS

Cell culture

Caco-2 cells were cultured in Minimal Essential Medium (Sigma) supplemented with nonessential amino acids and 10% heat-inactivated fetal bovine serum. For the differentiation assay, cells were seeded onto collagen-coated plate, and growth medium was changed every 3 d. HeLa S3 and 293 cells were cultured in Dulbecco's modified Eagle medium (Sigma) supplemented with 10% heat-inactivated fetal bovine serum.

RNA extraction, reverse transcription, and real-time quantitative PCR

Total RNA extraction was performed using miReasy mini kit with DNase I treatment (Qiagen). For detection of differentiation markers, LPH and SI, total RNAs were reverse transcribed by QuantiTect Reverse Transcription Kit (Qiagen). Semi-quantitative PCR was performed using LA Taq (Takara) with specific primer sets as follows:

LPH primer F 5′-TTTCTGTACGGACGGTTTCC-3′ and
LPH primer R 5′-AGAAAACGTGTCCCAAATGC-3′;
SI primer F 5′-AATCAGATGGCACAGGGTTC-3′ and
SI primer R 5′-TTCCTTTCCCCCATACATGA-3′;
GAPDH primer F 5′-GAAGGTCGGAGTCAACGGATTT-3′ and
GAPDH primer R 5′-ATGGGTGGAATCATATTGGAA-3′.

Quantification of mature miRNAs was performed by TaqMan miRNA assays Human Panel–Early Access Kit (Applied Biosystems) according to the manufacturer's instruction. As the kit did not contain probes for miR-192, data for miR-192 are not included in Figure 1B. Quantification of individual miRNAs (Fig. 2D) was performed by a TaqMan miRNA assay kit (Applied Biosystems).

Northern blot

To synthesize DIG-labeled RNA probe, vectors were constructed by inserting the following oligonucleotides into pcDNA3:

For mature miR-194 detection, 5′-TCCACATGGAGTTGCTGTTACA-3′;
For pre-miR-194-1 detection, 5′-AACTCCATGTGGACTGTGTACCAATTTCCAGTGGAGATGC-3′; and

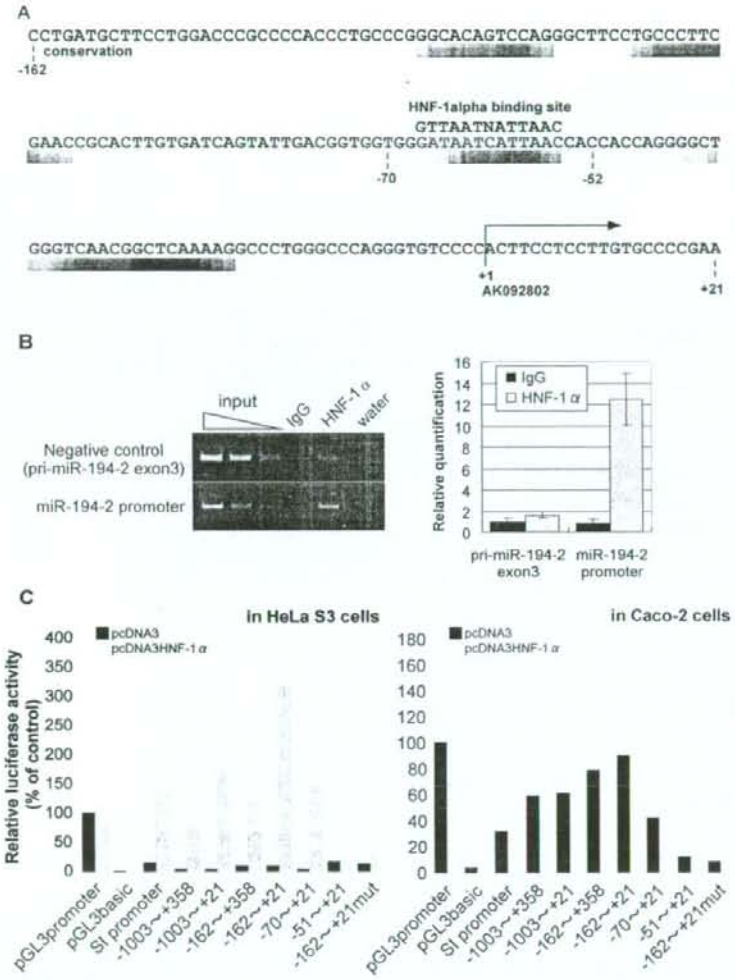

FIGURE 6. HNF-1α binds and regulates the miR-194-2 promoter in Caco-2 cells. (*A*) Sequence of pri-miR-194-2 promoter between −162 and +21. The region between −162 and +21 is partially conserved among human, mouse, and dog. Conserved sequences are indicated as density map (higher conservation becomes black). The transcription start site is indicated by an arrow. Consensus sequence of HNF-1α binding site is located at region between −67 and −55. (*B*) Chromatin immunoprecipitation (ChIP) analysis showing binding of HNF-1α to the miR-194-2 promoter in vivo in Caco-2 cells. Fixed chromatin from differentiated Caco-2 cells was prepared and immunoprecipitated either by anti HNF-1α antibody or normal goat IgG. ChIP primers were designed to amplify the region containing putative HNF-1α binding site in the pri-miR-194-2 promoter. Negative control primers were designed to amplify exon 3 of the pri-miR-194-2. PCR products were separated by acrylamide gel electrophoresis and stained by EtBr (*left*). Results of the quantitative PCR are shown as the relative amount of precipitated chromatin, in which chromatin precipitated by goat-IgG is set to 1. (*C*) Human pri-miR-194-2 promoter activity is up-regulated by forced expression of HNF-1α. Various luciferase reporter plasmids were cotransfected with either pcDNA3 mock vector (black bar) or HNF-1α expression vector (open bar) into HeLa S3 cells (*left*), or Caco-2 cells (*right*). SI-promoter contains promoter sequence of the sucrase-isomaltase (SI) gene, which is formerly reported to be up regulated by HNF-1α. Luciferase activities were normalized by *Renilla* luciferase activities.

For pre-miR-194-2 detection, 5′-AACTCCA TGTGGAAGTGCCCACTGGTTCCAGT GGGGCTGC-3′.

DIG-labeled RNA probes were synthesized by DIG RNA labeling kit (Roche). For pre-miRNA detection, knockdown of Dicer was performed before RNA extraction, using siRNA. The Dicer siRNA was transfected into cells by LipofectAmine2000 (Invitrogen). The sequence of the Dicer siRNA was as follows:

Dicer siRNA sense, 5′-UGCUUGAAGCAG CUCUGGAdTdT; and
Dicer siRNA anti-sense, 5′-UCCAGAGCU GCUUCAAGCAdTdT.

The letters "dT" represent deoxythymidine. Thirty micrograms of total RNA was separated by 8 M urea PAGE and transferred to Nybond N+ (GE Healthcare). After UV cross-linking, the membrane was hybridized with DIG-labeled probes in hybridization buffer (50% formamide, 5× SSC, 0.1% SDS, 2× Denhardt's solution, and salmon sperm DNA). Detections were achieved by AP-conjugated anti-DIG antibody (Roche) and CDP-star (GE Healthcare).

RT-PCR for pri-miRNA

Pri-miRNA cluster detection PCR was performed using Quantitect SYBR PCR kit (Qiagen) with specific sets of primers as follows:

pri-miR-194-1 F, 5′-AGCGTTTCAAATCT ACCAGT-3′;
pri-miR-194-1 R, 5′-TATCTTCTGTGTACC TGCCA-3′;
pri-miR-194-2 F, 5′-ATGATAAGAAGCCT CGGTGA-3′; and
pri-miR-194-2 R, 5′-GTGGGACCATGAGT GCTGCA-3′.

AK092802 and miRNA cluster RT-PCR (Fig. 3B) was performed with the following primers, and the sequence of the detected PCR products were confirmed by direct sequencing. Forward primer downstream of the transcription start site (DTSS F) was 5′-TTCCTCCTTGTGCCCCGAAG-3′, and pri-miR-194-2 R was used as the reverse primer (this primer is placed within the second intron). Template cDNA was prepared by reverse-transcription by SuperScript II (Invitrogen) using oligo dT primer.

RT-PCR for pri-miR-194-2 entire transcript (Fig. 4C) was performed with the following primers, Forward primer was DTSS F, and reverse primer was; 5′-CATCCCAGCCA CAGAGCATC-3′.

RACE analysis

5′ RACE was performed using GeneRacer kit (Invitrogen) according to manufacturer's protocol, except for the use of random primer in reverse transcription. PCR amplification of 5′ end of pri-miR-194-2 was performed by touchdown PCR by LA Taq (Takara) using GeneRacer 5′ primer and reverse primer 5′-CAGCAGGCA TTTTGGGAGAC-3′. Amplified 5′ RACE fragments were cloned into pGEM T-Easy (Promega) for sequence analysis. 3′ RACE was also performed using GeneRacer kit (Invitrogen). PCR Amplification of the 3′ end of pri-miR-194-2 was also performed using the gene-specific forward primer 5′-TTCCTCCTTGTGCCCCGAAG-3′ and GeneRacer 3′ primer. Amplified 3′ RACE fragments were also cloned into pGEM T-Easy (Promega) for sequence analysis.

Vector constructions

miRNA expression vectors were constructed by cloning miRNA coding region into pcDNA3.1(−) (Invitrogen). miRNA coding regions were amplified by Phusion DNA polymerase (New England Biolab) from Caco-2 genomic DNA using primers as follows:

miR-194-1cluster F, 5′-ATACTCGAGTAGAACATGAATAAATC GAGAC-3′;
miR-194-1cluster R, 5′-TATGAATTCTTACTCAATACATTTA CATGGTAG-3′;
miR-194-2cluster F, 5′-ATACTCGAGCCTGGGGCCACGAAGAC TGG-3′; and
miR-194-2cluster R, 5′-ATAGGATCCGGGGAATGAGACAGAG GGAGG-3′.

miR-194-2 promoter deletion variants were amplified by the following primers and cloned into pGL3basic between XhoI-MluI sites. Cloning primers were as follows:

−1003 primer F, 5′-ATGCACGCGTATGTCACCACCAGGGGT CGC-3′;
−162 primer F, 5′-ATGCACGCGTCCTGATGCTTCCTGGACCCG-3′;
−70 primer F, 5′-ATGCACGCGTTGGGATAATCATTAACCACC-3′;
−51 primer F, 5′-ATGCACGCGTCACCAGGGGCTGGGTCAACG-3′;
+21 primer R, 5′-TCGACTCGAGTTCGGGGCACAAGGAGGAA G-3′; and
+358 primer R, 5′-TCGACTCGAGACTCAGCCTGGCGGCCCTTC-3′.

Scrambled mutation was induced using Scrambled F 5′-GATAC TAACGTAAGCCACCAGGGGCTGGGT-3′ and Scrambled R 5′-ACGTTAGTATCATAGCCACCGTCAATACTG-3′. HNF-1α expression vector was constructed by cloning HNF-1α cDNA into pcDNA3 (Invitrogen). HNF-1α primers were 5′-ATG CAAGCTTGCCACCATGGTTTCTAAACTGAGCCAGC-3′ and 5′-TAATGAATTCTTACTGGGAGGAAGAGGCCA-3′.

Transfection and luciferase assay

Transfections were performed using LipofectAmine2000 (Invitrogen) according to the manufacturer's protocol. For examination of miRNA generation, miRNA expression vector, luciferase miRNA-sensor vector, and pRL-TK were mixed (10:9:1), and cotransfected into cells were cultured in 96-well plate. For examination of miRNA promoter activity, the HNF-1α expression vector, luciferase miRNA promoter vector, and pRL-TK were mixed (20:19:1) and cotransfected into cells cultured in 96-well plate. Luciferase activity was measured by the Dual luciferase assay kit (Promega).

ChIP assay

To cross-link chromatin, differentiated Caco-2 cells were treated with 1% formaldehyde for 10 min at room temperature. Cross-linking was stopped by addition of 0.125 M glycine. After being washed twice with ice-cold PBS, cells were resuspended in NP-40 nuclear extraction buffer (10 mM HEPES at pH 7.5, 10 mM NaCl, 3 mM $MgCl_2$, 0.5% NP-40, and protease inhibitor) and centrifuged at 3000 rpm for 10 min. Crude nuclei were resuspended in SDS lysis buffer (1% SDS, 10 mM EDTA, 50 mM Tris-HCl at pH 8.0, and protease inhibitor), and extensively sonicated by Bioruptor. Sonicated chromatin was centrifuged at 15,000 rpm, and the supernatant was collected (input control). The supernatant was mixed with 9 vol of ChIP dilution buffer (11 mM Tris/HCl at pH 8.0, 154 mM NaCl, 1 mM EDTA, 0.5 mM EGTA, 1.1% Triton X-100, 0.11% sodium deoxycholate, and protease inhibitors) and precleared with preblocked Protein G–Sepharose (GE Healthcare). Precleared chromatin was immunoprecipitated with 5 μg of anti-HNF-1α antibody (Santa Cruz, sc-6547) or 5 μg of normal goat IgG (Vector Laboratory, I-5000), and the immuno complexes were collected by preblocked Protein G–Sepharose. The beads were washed sequentially by RIPA, RIPA containing 500 mM NaCl, LiCl wash buffer, and twice by TE. Collected chromatin were eluted in ChIP elution buffer (1% SDS, 100 mM $NaHCO_3$), adjusted to 200 mM NaCl, and incubated for at least 6 h at 65°C to reverse cross-link. After treatment with RNase A (Nippongene) and Proteinase K (Roche), DNA fragments were extracted by phenol/chloroform and ethanol precipitation. Quantitative PCR was performed with Quantitect SYBR PCR kit (Qiagen) using the following primers: miR-194-2 promoter ChIP primer F, 5′-TGATCAGTATTGACGGTGGTG-3′; primer R, 5′-AAGGAGGAAGTGGGGACAC-3′. Also used were negative control (exon3 of pri-miR-194-2) primer F, 5′-CCCACTGAC CTGTGTCCTTT-3′; primer R, 5′-AGAGGGGTTGGAGGTGAG AC-3′. Detected PCR products were sequenced after cloning into pGEM T-Easy vector (Promega).

ACKNOWLEDGMENTS

This study was supported in part by grants-in-aid for Scientific Research, Scientific Research on Priority Areas, Exploratory Research, and Creative Scientific Research from the Japanese Ministry of Education, Culture, Sports, Science and Technology; the Japanese Ministry of Health, Labor and Welfare; and the Japan Medical Association.

Received September 3, 2007; accepted March 12, 2008.

REFERENCES

Ambros, V. 2004. The functions of animal microRNAs. *Nature* **431:** 350–355.
Bartel, D.P. 2004. MicroRNAs: Genomics, biogenesis, mechanism, and function. *Cell* **116:** 281–297.
Boudreau, F., Zhu, Y., and Traber, P.G. 2001. Sucrase-isomaltase gene transcription requires the hepatocyte nuclear factor-1 (HNF-1)

regulatory element and is regulated by the ratio of HNF-1α to HNF-1β. *J. Biol. Chem.* **276:** 32122–32128.

Boudreau, F., Rings, E.H., van Wering, H.M., Kim, R.K., Swain, G.P., Krasinski, S.D., Moffett, J., Grand, R.J., Suh, E.R., and Traber, P.G. 2002. Hepatocyte nuclear factor-1α, GATA-4, and caudal related homeodomain protein Cdx2 interact functionally to modulate intestinal gene transcription. Implication for the developmental regulation of the sucrase-isomaltase gene. *J. Biol. Chem.* **277:** 31909–31917.

Brennecke, J., Hipfner, D.R., Stark, A., Russell, R.B., and Cohen, S.M. 2003. bantam encodes a developmentally regulated microRNA that controls cell proliferation and regulates the proapoptotic gene hid in *Drosophila*. *Cell* **113:** 25–36.

Cai, X., Hagedorn, C.H., and Cullen, B.R. 2004. Human microRNAs are processed from capped, polyadenylated transcripts that can also function as mRNAs. *RNA* **10:** 1957–1966.

Chen, C.Z., Li, L., Lodish, H.F., and Bartel, D.P. 2004. MicroRNAs modulate hematopoietic lineage differentiation. *Science* **303:** 83–86.

Chen, J.F., Mandel, E.M., Thomson, J.M., Wu, Q., Callis, T.E., Hammond, S.M., Conlon, F.L., and Wang, D.Z. 2006. The role of microRNA-1 and microRNA-133 in skeletal muscle proliferation and differentiation. *Nat. Genet.* **38:** 228–233.

Cheng, A.M., Byrom, M.W., Shelton, J., and Ford, L.P. 2005. Antisense inhibition of human miRNAs and indications for an involvement of miRNA in cell growth and apoptosis. *Nucleic Acids Res.* **33:** 1290–1297.

Cimmino, A., Calin, G.A., Fabbri, M., Iorio, M.V., Ferracin, M., Shimizu, M., Wojcik, S.E., Aqeilan, R.I., Zupo, S., Dono, M., et al. 2005. miR-15 and miR-16 induce apoptosis by targeting BCL2. *Proc. Natl. Acad. Sci.* **102:** 13944–13949.

Clarke, A.R. 2006. Wnt signalling in the mouse intestine. *Oncogene* **25:** 7512–7521.

Crosnier, C., Stamataki, D., and Lewis, J. 2006. Organizing cell renewal in the intestine: Stem cells, signals and combinatorial control. *Nat. Rev. Genet.* **7:** 349–359.

Esau, C., Kang, X., Peralta, E., Hanson, E., Marcusson, E.G., Ravichandran, L.V., Sun, Y., Koo, S., Perera, R.J., Jain, R., et al. 2004. MicroRNA-143 regulates adipocyte differentiation. *J. Biol. Chem.* **279:** 52361–52365.

Fre, S., Huyghe, M., Mourikis, P., Robine, S., Louvard, D., and Artavanis-Tsakonas, S. 2005. Notch signals control the fate of immature progenitor cells in the intestine. *Nature* **435:** 964–968.

Giraldez, A.J., Cinalli, R.M., Glasner, M.E., Enright, A.J., Thomson, J.M., Baskerville, S., Hammond, S.M., Bartel, D.P., and Schier, A.F. 2005. MicroRNAs regulate brain morphogenesis in zebrafish. *Science* **308:** 833–838.

Gregorieff, A. and Clevers, H. 2005. Wnt signaling in the intestinal epithelium: From endoderm to cancer. *Genes & Dev.* **19:** 877–890.

He, L., He, X., Lim, L.P., de Stanchina, E., Xuan, Z., Liang, Y., Xue, W., Zender, L., Magnus, J., Ridzon, D., et al. 2007. A microRNA component of the p53 tumour suppressor network. *Nature* **447:** 1130–1134.

Hu, C. and Perlmutter, D.H. 1999. Regulation of α1-antitrypsin gene expression in human intestinal epithelial cell line caco-2 by HNF-1α and HNF-4. *Am. J. Physiol.* **276:** G1181–G1194.

Hu, C. and Perlmutter, D.H. 2002. Cell-specific involvement of HNF-1β in α(1)-antitrypsin gene expression in human respiratory epithelial cells. *Am. J. Physiol. Lung Cell. Mol. Physiol.* **282:** L757–L765.

Jing, Q., Huang, S., Guth, S., Zarubin, T., Motoyama, A., Chen, J., Di Padova, F., Lin, S.C., Gram, H., and Han, J. 2005. Involvement of microRNA in AU-rich element-mediated mRNA instability. *Cell* **120:** 623–634.

Kato, M., Zhang, J., Wang, M., Lanting, L., Yuan, H., Rossi, J.J., and Natarajan, R. 2007. MicroRNA-192 in diabetic kidney glomeruli and its function in TGFβ-induced collagen expression via inhibition of E-box repressors. *Proc. Natl. Acad. Sci.* **104:** 3432–3437.

Kim, Y.K. and Kim, V.N. 2007. Processing of intronic microRNAs. *EMBO J.* **26:** 775–783.

Kim, H.K., Lee, Y.S., Sivaprasad, U., Malhotra, A., and Dutta, A. 2006. Muscle-specific microRNA miR-206 promotes muscle differentiation. *J. Cell Biol.* **174:** 677–687.

Krasinski, S.D., Van Wering, H.M., Tannemaat, M.R., and Grand, R.J. 2001. Differential activation of intestinal gene promoters: Functional interactions between GATA-5 and HNF-1α. *Am. J. Physiol.* **281:** G69–G84.

Krutzfeldt, J., Rajewsky, N., Braich, R., Rajeev, K.G., Tuschl, T., Manoharan, M., and Stoffel, M. 2005. Silencing of microRNAs in vivo with "antagomirs." *Nature* **438:** 685–689.

Lagos-Quintana, M., Rauhut, R., Meyer, J., Borkhardt, A., and Tuschl, T. 2003. New microRNAs from mouse and human. *RNA* **9:** 175–179.

Lee, Y., Kim, M., Han, J., Yeom, K.H., Lee, S., Baek, S.H., and Kim, V.N. 2004. MicroRNA genes are transcribed by RNA polymerase II. *EMBO J.* **23:** 4051–4060.

Mendel, D.B. and Crabtree, G.R. 1991. HNF-1, a member of a novel class of dimerizing homeodomain proteins. *J. Biol. Chem.* **266:** 677–680.

Mitchelmore, C., Troelsen, J.T., Sjostrom, H., and Noren, O. 1998. The HOXC11 homeodomain protein interacts with the lactase-phlorizin hydrolase promoter and stimulates HNF1α-dependent transcription. *J. Biol. Chem.* **273:** 13297–13306.

Olsen, P.H. and Ambros, V. 1999. The lin-4 regulatory RNA controls developmental timing in *Caenorhabditis elegans* by blocking LIN-14 protein synthesis after the initiation of translation. *Dev. Biol.* **216:** 671–680.

Sancho, E., Batlle, E., and Clevers, H. 2004. Signaling pathways in intestinal development and cancer. *Annu. Rev. Cell Dev. Biol.* **20:** 695–723.

Schroder, O., Hess, S., Caspary, W.F., and Stein, J. 1999. Mediation of differentiating effects of butyrate on the intestinal cell line Caco-2 by transforming growth factor-β1. *Eur. J. Nutr.* **38:** 45–50.

Stanger, B.Z., Datar, R., Murtaugh, L.C., and Melton, D.A. 2005. Direct regulation of intestinal fate by Notch. *Proc. Natl. Acad. Sci.* **102:** 12443–12448.

Taganov, K.D., Boldin, M.P., Chang, K.J., and Baltimore, D. 2006. NF-κB-dependent induction of microRNA miR-146, an inhibitor targeted to signaling proteins of innate immune responses. *Proc. Natl. Acad. Sci.* **103:** 12481–12486.

Thomson, J.M., Newman, M., Parker, J.S., Morin-Kensicki, E.M., Wright, T., and Hammond, S.M. 2006. Extensive post-transcriptional regulation of microRNAs and its implications for cancer. *Genes & Dev.* **20:** 2202–2207.

van Wering, H.M., Huibregtse, I.L., van der Zwan, S.M., de Bie, M.S., Dowling, L.N., Boudreau, F., Rings, E.H., Grand, R.J., and Krasinski, S.D. 2002. Physical interaction between GATA-5 and hepatocyte nuclear factor-1α results in synergistic activation of the human lactase-phlorizin hydrolase promoter. *J. Biol. Chem.* **277:** 27659–27667.

Viswanathan, S.R., Daley, G.Q., and Gregory, R.I. 2008. Selective blockade of microRNA processing by Lin-28. *Science* **320:** 97–100.

Wang, L., Klopot, A., Freund, J.N., Dowling, L.N., Krasinski, S.D., and Fleet, J.C. 2004. Control of differentiation-induced calbindin-D9k gene expression in Caco-2 cells by cdx-2 and HNF-1α. *Am. J. Physiol.* **287:** G943–G953.

Wienholds, E., Kloosterman, W.P., Miska, E., Alvarez-Saavedra, E., Berezikov, E., de Bruijn, E., Horvitz, H.R., Kauppinen, S., and Plasterk, R.H. 2005. MicroRNA expression in zebrafish embryonic development. *Science* **309:** 310–311.

Wightman, B., Ha, I., and Ruvkun, G. 1993. Posttranscriptional regulation of the heterochronic gene lin-14 by lin-4 mediates temporal pattern formation in *C. elegans*. *Cell* **75:** 855–862.

Wu, G.D., Chen, L., Forslund, K., and Traber, P.G. 1994. Hepatocyte nuclear factor-1α (HNF-1α) and HNF-1β regulate transcription via two elements in an intestine-specific promoter. *J. Biol. Chem.* **269:** 17080–17085.

Zamore, P.D. and Haley, B. 2005. Ribo-gnome: The big world of small RNAs. *Science* **309:** 1519–1524.

Human Neutrophil Peptides 1–3 Are Useful Biomarkers in Patients with Active Ulcerative Colitis

Shuji Kanmura, MD, Hirofumi Uto, MD,* Masatsugu Numata, MD,† Shinichi Hashimoto, MD,* Akihiro Moriuchi, MD,* Hiroshi Fujita, MD,* Makoto Oketani, MD,* Akio Ido, MD,* Mayumi Kodama, MD,‡ Hidehisa Ohi, MD,§ and Hirohito Tsubouchi, MD,**

Background: A specific useful biomarker for diagnosing ulcerative colitis (UC) has not yet been described. This study employed proteomics to identify serum protein biomarkers for UC.

Methods: Ninety-four blood samples were isolated from patients and controls (including 48 UC, 22 Crohn's disease [CD], 5 colorectal cancer, and 6 infectious colitis patients and 13 healthy subjects). Serum samples were analyzed using the SELDI-TOF/MS ProteinChip system. After applying the samples to ProteinChip arrays, we assessed differences in the proteomes using Ciphergen ProteinChip software and identified candidate proteins, which were then characterized in immunoassays.

Results: Preliminary analysis using the ProteinChip system revealed significant peak-intensity differences for 27 serum proteins between 11 patients with UC and 7 healthy subjects. Among these proteins, 3 proteins (with mass/charge ratios of approximately 3400) were identified as human neutrophil peptides 1–3 (HNP 1–3). The presence of HNP 1–3 in the patient sera was confirmed using immunoassays. Enzyme-linked immunosorbent assays demonstrated that the mean plasma concentration of HNP 1–3 was significantly higher in patients with active UC ($n = 28$) than in patients whose UC was in remission ($n = 20$) or patients with CD ($n = 22$), infectious colitis, or healthy subjects, and tended to be higher than in patients with colon cancer. In addition, the plasma concentration of HNP 1–3 in patients that responded to corticosteroids-based therapy decreased after treatment, whereas it was not changed in nonresponders.

Conclusions: HNP 1–3 is a novel biomarker that may be useful for diagnosing patients with active UC and predicting treatment outcomes.

(Inflamm Bowel Dis 2008;00:000–000)

Key Words: biomarkers, inflammatory bowel disease, ulcerative colitis, human neutrophil peptides 1–3, SELDI-TOF/MS, proteomics

Genetic and environmental factors contribute to the disease process of inflammatory bowel disease (IBD), including ulcerative colitis (UC).[1,2] The presence of active inflammation of the gut in patients with UC is associated with an acute-phase reaction and the migration of leukocytes to the gut. This, in turn, promotes the production of a large number of proteins.[3] Determination of inflammatory activity is important for the comprehensive assessment of patients with UC and for the tailoring of therapy.[4] Many clinical activity indices are used to stratify patients with UC. For example, the UC Disease Activity Index (UCDAI)[5] is a widely used measure of clinical parameters of disease activity. These indices, however, only provide indirect assessments of disease activity. Whereas albumin, hemoglobin, the erythrocyte sedimentation rate (ESR), and acute-phase protein levels are commonly used biological parameters for assessing UC, there are no accurate markers to assess the inflammatory activity observed with histopathologic or endoscopic analyses.[6]

Proteomic array technology, in which a ProteinChip system is coupled with surface-enhanced laser desorption ionization/time-of-flight/mass spectrometry (SELDI-TOF/MS) for the profiling of serum or plasma, is a powerful tool that allows the identification of new biomarkers for malignant tumors and autoimmune diseases.[7,8] This technology is a rapid and sensitive technique, in which the detected peak intensities for some proteins correlate with concentrations determined using enzyme-linked immunosorbent assay (ELISA). Novel blood biomarkers which are identified by this proteomics, may provide clinicians with more accurate parameters to assess inflammatory activity in UC.

Received for publication October 29, 2008; Accepted November 14, 2008.

From the *Digestive Disease and Life-style Related Disease Health Research, Human and Environmental Sciences, Kagoshima University Graduate School of Medical and Dental Sciences, Kagoshima, Japan, †Department of Experimental Therapeutics, Translational Research Center, Kyoto University Hospital, Kyoto, Japan, ‡Division of Gastroenterology and Hematology, Department of Internal Medicine, Faculty of Medicine, University of Miyazaki, Miyazaki, Japan, §Division of Gastroenterology, Imamura Hospital, Kagoshima, Japan.

Supported in part by grants-in-aid to the Research Committee of Inflammatory Bowel Disease from the Ministry of Health, Labour and Welfare of Japan.

Reprints: Hirofumi Uto, 8-35-1 Sakuragaoka, Kagoshima, Kagoshima, 890-8520, Japan (e-mail: hirouto@m2.kufm.kagoshima-u.ac.jp).

DOI 10.1002/ibd.20854

Published online in Wiley InterScience (www.interscience.wiley.com).

Host defense processes, which rely on both innate and adaptive immune mechanisms, are critical for the development of IBD.[1,2] Innate immunity participates in the activation of antigen-specific adaptive immune responses, including the production of antimicrobial peptides/proteins. In mammals, defensins, a class of antimicrobial peptides, can be divided into 2 major groups: α-defensins and β-defensins.[9] Six types of α-defensins have been identified, 4 of which are produced predominantly by neutrophils and phagocytes and stored in the granules of these cell types (denoted human neutrophil peptides 1–4; HNP 1–4). The remaining 2 α-defensins are localized in Paneth cell granules (denoted human α-defensins 5 and 6; HD 5 and 6). Although the amino-acid sequences of HNP 1, HNP 2, and HNP 3 are very similar, the sequence of HNP 4 is different than those of HNP 1–3. HD 5 is expressed by metaplastic Paneth cells in the colons of patients with UC or CD. The expression levels of HD 5 in blood, however, have not been examined; there are currently no data evaluating HNP 1–3 expression in patients with IBD.

In this study we clearly demonstrate serum profiling with increased levels of HNP 1–3 in the sera of patients with UC using a proteomics-based approach. We also compared the protein levels of HNP 1–3 in plasma samples from patients with UC and Crohn's disease (CD), before and after treatment for UC, and in patients in which treatment was effective or not effective. These analyses will contribute to our understanding of the pathogenesis of UC and aid in the discovery novel biomarkers to assess disease activity and therapeutic responses.

MATERIALS AND METHODS

Patients

After obtaining written informed consent, we analyzed a total of 94 blood samples from patients with IBD, colorectal cancer (CRC), infectious colitis, and control subjects. Forty-eight patients were diagnosed with UC (20 females and 28 males; median age, 39 years; age range, 12–72 years) and 22 with CD (11 females and 11 males; 29 years; 16–57 years). The control group contained 13 healthy subjects (5 females and 8 males; median age 30 years; age range, 24–34 years) and 5 with CRC (1 female and 4 males; median age 62 years; age range, 52–80 years) and 6 with infectious colitis (3 females and 3 males; median age 42 years; age range, 17–77 years). The study protocol was approved by the Ethics Committee of the Kagoshima University Graduate School of Medical and Dental Sciences (Kagoshima, Japan) and the Faculty of Medicine at the University of Miyazaki (Miyazaki, Japan). All IBD patients were diagnosed using established endoscopic, radiological, histological, and clinical criteria. The inactive or remission phase of UC was defined as a UCDAI score less than or equal to 2, whereas the active phase was defined as a UCDAI score greater than or equal to 3.[5] Twenty and 28 patients with UC were identified as inactive-phase and active-phase patients, respectively. All of the patients with active-phase UC were treated with oral corticosteroids, whereas 23 received leukocytapheresis therapy (LCAP) (Table 1). Furthermore, 4 of the active UC patients did not respond to treatment and eventually underwent a total colectomy. Fourteen patients with CD had high disease activities based on an International Organization for the Study of Inflammatory Bowel Disease (IOIBD) score of 2 or greater[10] and were regarded as active-phase patients. Eight patients that had lower IOIBD scores (0 or 1) were defined as inactive-phase patients. All 5 CRC patients were diagnosed with Duke's A group cancers by endoscopic, radiological, and histological examinations. All 6 patients with infectious colitis had diarrhea and fever, and were diagnosed based on clinical findings.

SELDI-TOF/MS

We used chips with cationic surfaces for analysis (CM10; Bio-Rad Laboratories, Hercules, CA). Serum samples were denatured in urea buffer (7 M urea, 2 M thiourea, 4% CHAPS, 1% dithiothreitol, and 2% ampholites), and then diluted 1:9 in binding/washing buffer (50 mM sodium acetate, pH 4). After washing the chip twice in binding/washing buffer, we applied 100 μL of diluted serum to each chip spot. Samples were incubated for 40 minutes and washed 3 times. After rinsing the chips once in water, 0.5 μL CHCA (α-cyano-4-hydoroxycinnamic acid; Nacalai Tesque, Kyoto, Japan) was applied twice to each spot and allowed to air-dry. Arrays were analyzed using a ProteinChip Reader (ProteinChip Biology System II; Bio-Rad Laboratories). TOF spectra were generated with laser shots collected in positive mode. The laser intensity ranged from 190 to 195 with a detector sensitivity of 6. On average, 65 laser shots per spectrum were used. A mixture of standard mass calibrant proteins (All-in-one Peptide Standard; Bio-Rad Laboratories) in 500 nL was used to calibrate the system for mass accuracy. The standards were applied to a single spot of the normal phase chip array (NP20; Bio-Rad Laboratories), after which two 1.0-μL samples of saturated CHCA were applied. TOF values were compared to the molecular masses of the standard proteins; calibration was performed according to the manufacturer's instructions.[7]

Immunodepletion Assay

Initially, 6 μL of anti-HNP 1–3 antibody solution (120 ng; Hycult Biotechnology, Netherlands) was bound to 30 μL of Protein A–agarose (Sigma Chemical, St. Louis, MO) for 15 minutes on ice. The postcentrifugation supernatant was discarded and the pellet was washed twice in buffer containing 20 mM HEPES (pH 7.8), 25 mM KCl, 5 mM $MgCl_2$, 0.1 mM EDTA, and 0.05% NP40. Then 15 μL of sera from each patient with UC was incubated with a pellet for 45 minutes on ice. As a negative control, samples were incubated with

TABLE 1. Characteristics of Patients with UC or CD

	UC		CD	
Disease activity[a]	Active	Inactive	Active	Inactive
Number	28	20	14	8
Gender (M/F)	19/9	9/11	10/4	6/2
Age (range), yr	41 ± 16 (14–68)	31 ± 16 (12–72)	32 ± 13 (16–57)	28 ± 7 (18–40)
Disease duration (range), yr	5.6 ± 4.8 (1–19)	5.2 ± 4.3 (1–18)	9.4 ± 7.4 (3–22)	6.0 ± 3.8 (1–13)
Treatment[b]				
5-aminosalicylic acid	28	19	14	8
Corticosteroid	28	7	10	2
Leukocytapheresis	23	0	0	0
Type of UC				
Left-side colitis	4	8	—	—
Pancolitis	24	12	—	—
Type of CD				
Ileal	—	—	4	2
Ileocolonic	—	—	9	5
Colonic	—	—	1	1

UC, ulcerative colitis; CD, Crohn's disease. Data are shown as the means ± SD or range.
[a]Active UC is defined as an Ulcerative Colitis Disease Activity Index score equal to or greater than 3, and active CD is defined as an International Organization for the Study of Inflammatory Bowel Disease score equal to or greater than 2.
[b]Includes the overlap treatment.

Protein A–agarose in the absence of a specific antibody. After incubation, samples were cleared by centrifugation; 3 μL of each supernatant was analyzed on NP20 ProteinChip arrays using a PBS II reader.[11]

ELISA

We determined the HNP 1–3 (P59665, P59666) concentrations in plasma using a human HNP 1–3 ELISA kit (Hycult Biotechnology) according to the manufacturer's instructions. Samples were analyzed in duplicate using a plate reader (Bio-Rad Laboratories) at 450 nm. The concentration of each protein in the plasma was calculated according to a standard curve.

Immunohistochemical Studies

HNP 1–3 expression in colon tissue was evaluated using immunohistochemistry. Abnormal colon tissues were obtained by total colectomy in patients with UC, whereas normal colon tissues were isolated in surgical resections for colon cancer by taking surrounding normal tissue without malignant cells. Colon tissues were fixed in 10% formalin and embedded in paraffin. For histological examination, 5-μm slices were stained with hematoxylin and eosin (HE). The anti-HNP 1–3 monoclonal antibodies (BMA Biochemicals, Augst, Switzerland) was diluted to a final concentration of 0.5% (w/v) in phosphate-buffered saline (PBS) supplemented with 1% fetal bovine serum (FBS). Immunohistochemical analysis of paraffin-embedded sections using antibodies against HNP 1–3 was performed as described.[12] EnVision plus horseradish peroxidase (Dako, Carpinteria, CA) was applied to samples; chromatin 3′,3′-diaminobenzidine was used to detect bound antibody.

Statistical Analysis

Values shown are the means ± SD. Statistical significance, including that for differences in laboratory data and individual peaks in SELDI-TOF/MS, was determined using Mann–Whitney *U*- and paired *t*-tests. *P*-values < 0.05 were considered to be statistically significant. The discriminatory power for each putative marker was described via the area under the curve (AUC) from receiver operating characteristic (ROC) analysis. The statistical analyses were performed using StatView 4.5 software (Abacus Concepts, Berkeley, CA), SPSS software (SPSS, Chicago, IL), and Ciphergen ProteinChip Software (Fremont, CA) v. 3.0.2.

RESULTS

Profiling Serum Proteins in Patients with UC

We performed differential profiling of serum proteins in 11 patients with UC and 7 normal healthy controls using the SELDI ProteinChip system. Peaks were automatically detected using Ciphergen ProteinChip Software 3.0.2.[7,13] Twenty-seven serum peaks in the 3000–10,000 m/z range

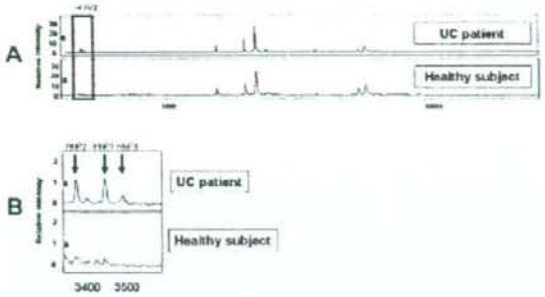

Figure 1. Serum proteomics of UC patients and healthy controls using SELDI-TOF/MS. (A) Spectra representing the serum proteins of a patient with UC and a healthy volunteer. The horizontal axis shows a range from 3000 to 10,000 m/z. Significant differences in peak intensities between patients with UC and healthy volunteers were found for 27 peaks. (B) The intensities of the protein peaks are shown for the range between 3300 and 3600 m/z. Protein peaks with m/z values of 3371, 3443, and 3486 represent HNP 2, HNP 1, and HNP 3, respectively.

were significantly different between the 2 patient groups (Fig. 1). Sixteen peaks resulted in *P*-values less than 0.01 (Table 2). The most dramatic difference was detected for a 3371 m/z protein, the level of which was increased in the sera of UC patients compared with healthy controls.

Identification of HNP 1–3

A previous study of colon tumor tissue identified a similarly increased signal at 3371 m/z using ProteinChip

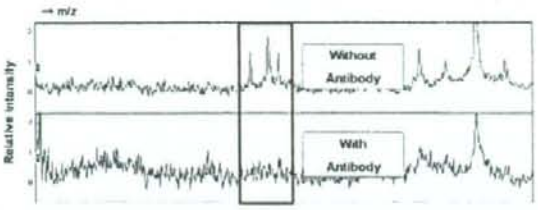

Figure 2. Immunodepletion assay using Protein A beads. Anti-HNP 1–3 antibodies (Hycult Biotechnology) were bound to 30 μL of Protein A beads. Sera from UC patients were incubated with these beads. After clearing by centrifugation, 3 μL of each supernatant was analyzed using an NP20 ProteinChip array.

arrays.[12,14] The peak was confirmed to correspond to HNP 2 with an immunodepletion assay. Peaks at 3443 and 3486 m/z, reported to correspond to HNP 1 and HNP 3 in the previous report, were also found to be significantly increased in analyses of the sera of UC patients compared to results observed for control samples. HNP 1, 2, and 3 have similar structures consisting of 30, 29, and 30 amino acids, respectively; 29 of the amino acids are identical among the peptides.[12,15] We also subjected the serum samples to immunodepletion assays using monoclonal antibodies against HNP 1–3 and found that the 3371, 3443, and 3486 m/z protein peaks in the SELDI-TOF MS spectra were no longer observed for the sera from patients with UC (Fig. 2). These peaks were clearly observed for negative control samples, which underwent immunodepletion assays in the absence of specific antibodies. These results indicate that the 3371, 3443, and 3486 m/z

TABLE 2. Discriminatory Peaks and Mean Values in Samples from Patients with Ulcerative Colitis and Healthy Volunteers

Mass to Charge (m/z)	Ulcerative Colitis (n = 11)	Healthy Subject (n = 7)	P-value
3371	1.42 ± 0.66	0.40 ± 0.10	4.8×10^{-4}
4789	0.51 ± 0.82	0.05 ± 0.03	4.8×10^{-4}
5421	0.34 ± 0.24	0.09 ± 0.02	4.8×10^{-4}
8688	0.65 ± 0.41	1.70 ± 0.38	6.8×10^{-4}
5838	0.79 ± 0.85	0.21 ± 0.05	9.4×10^{-4}
4351	0.82 ± 0.62	2.21 ± 0.56	1.3×10^{-3}
5620	0.11 ± 0.05	0.39 ± 0.23	1.7×10^{-3}
6881	1.00 ± 0.59	2.24 ± 0.46	1.7×10^{-3}
9358	0.17 ± 0.06	0.80 ± 0.52	1.7×10^{-3}
7023	0.12 ± 0.07	0.66 ± 0.46	2.4×10^{-3}
4469	3.31 ± 2.16	1.02 ± 0.59	3.2×10^{-3}
4542	0.39 ± 0.17	0.16 ± 0.02	4.3×10^{-3}
4590	0.86 ± 0.45	1.63 ± 0.26	4.3×10^{-3}
4287	0.68 ± 0.37	1.26 ± 0.39	5.7×10^{-3}
2900	0.18 ± 0.12	0.37 ± 0.14	9.8×10^{-3}
2979	1.00 ± 0.88	0.26 ± 0.15	9.8×10^{-3}

Statistical significance was determined using a Mann-Whitney *U*-test.

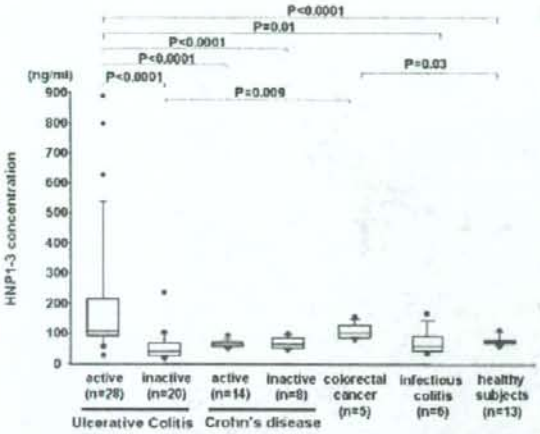

Figure 3. Concentrations of HNP 1–3 in the plasma of patients with UC, CD, colorectal cancer, infectious colitis, and healthy controls. Boxes indicate the median ± 25th percentile. The lower bar indicates the 10th percentile and the upper bar indicates the 90th percentile.

protein peaks, which were larger in the spectra for sera of UC patients, corresponded to HNP 1–3.

Concentrations of HNP 1–3 in Plasma

It was not possible to determine the individual concentrations of HNP 1, 2, or 3 using commercially available ELISA kits; therefore, we evaluated the total concentration of HNP 1, 2, and 3 in plasma. We found that there was a clear correlation between the serum HNP 1–3 peak intensities determined using the SELDI system and the plasma HNP 1–3 concentration measured using ELISAs in 11 patients with UC and 7 normal controls ($r = 0.68$, $P < 0.01$). We then determined the plasma concentrations of HNP 1–3 in 48 UC patients, 22 CD patients (Table 1), 5 CRC patients, 6 infectious colitis patients, and 13 healthy controls (Fig. 3). The plasma concentrations of HNP 1–3 were significantly higher in patients with active UC (203.1 ± 215.5 ng/mL) than in patients with inactive UC (58.3 ± 49.5 ng/mL), CD (active; 65.5 ± 11.2 ng/mL, inactive; 70.4 ± 20.0 ng/mL), infectious colitis (72.2 ± 16.5 ng/mL), or the healthy controls (77.5 ± 16.4 ng/mL). In addition, HNP 1–3 concentrations in patients with active UC tended to be higher in patients with CRC at Duke's stage A (100.8 ± 27.6 ng/mL), but not significantly. HNP 1–3 concentrations in CRC patients were also higher than those in patients with inactive UC and healthy controls.

Expression of HNP 1–3 in Intestinal Tissue

We examined the localization of HNP 1–3 in normal tissues and those from patients with active-phase CD or UC using immunohistochemistry. The colonic mucosa, lamina propria, muscle layer, and crypt abscesses of patients with active UC exhibited strong staining with anti-HNP 1–3 antibodies (Fig. 4). These sections contained a number of infiltrating neutrophils (Fig. 4B,C), which may provide a source of the secreted HNP 1–3 near the colonic epithelium. Positive staining for neutrophils, however, was seen in the blood vessels of both normal and abnormal colon tissues. In addition, small numbers of neutrophils with positive staining were seen in submucosal tissue of patients with CD (Fig. 4D). Epithelial cells in colon samples from patients with inflamed CD or from normal healthy subjects did not exhibit staining with anti-HNP 1–3 antibodies (Fig. 4D,E).

HNP 1–3 as a Biomarker in UC Patients

We investigated the association between the HNP 1–3 concentration and the clinical course of UC. We determined the HNP 1–3 concentrations in pairs of plasma samples from 15 patients with active UC obtained before and after induction therapy with corticosteroids (Table 3). Eight UC patients in the responder group were successfully treated by induction therapy. The elevated HNP 1–3 levels of UC patients in the responder group were reduced after induction therapy (Fig. 5). In contrast, 7 patients in the nonresponder group, 2 of whom had a total colectomy and 5 who quickly relapsed, were not effectively treated. The HNP 1–3 levels of patients in the nonresponder group before treatment were lower than those in the responder group and were not changed after treatment (Fig. 5). Additionally, although plasma HNP 1–3 levels (means ± SD) of responder active UC patients (273.0 ± 224.8 ng/mL) were higher than those with active CD (65.5 ± 11.2 ng/mL) ($P < 0.001$), those with nonresponder active UC (84.6 ± 26.5 ng/mL) were similar to those with active CD. These results indicate that patients with active UC and low HNP 1–3 levels do not respond well to treatment.

We evaluated the relationship between the HNP 1–3 levels and the clinical activity of UC. There was a significant correlation between the HNP 1–3 levels and the UCDAI score or the white blood cell count (WBC) of UC patients ($r = 0.54$, $P < 0.01$; $r = 0.55$, $P < 0.01$, respectively), although no correlation between the HNP 1–3 levels and the C-reactive protein (CRP) levels was noted ($r = 0.24$). In addition, ROC analysis was performed to estimate the efficiency of induction therapy for patients with active-phase UC; we calculated the sensitivity and specificity of HNP 1–3 levels for discriminating responder UC patients from nonresponders. We obtained a sensitivity of 89% and a specificity of 80% using a cutoff value of 100 ng/mL HNP 1–3; the ROC AUC was 0.89 between the responder and nonresponder groups of UC patients. For evaluations of the activity of UC, we compared such inflammatory markers as the CRP level and the WBC to the HNP 1–3 level in patients with UC. ROC AUC of the CRP level and WBC were 0.76 and 0.56, respectively. Thus,

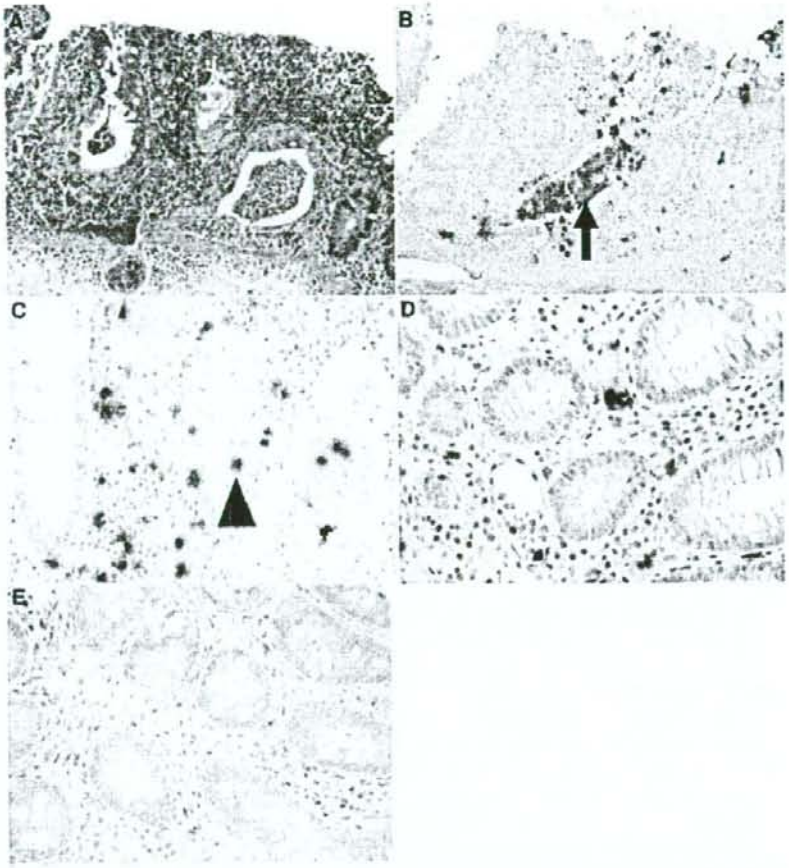

Figure 4. Expression of HNP 1–3 in the tissue of patients with active UC or CD and in normal colon tissue. (A) HE staining of colon tissues from patients with UC. (B,C) Immunohistochemical staining demonstrated extensive HNP 1–3 expression in the colon tissues of patients with UC. Many HNP 1–3-positive cells were observed in the crypt abscesses (B: arrow) and in neutrophils that had migrated into the epithelial layers (C: arrowhead). In addition, an ulcer lesion observed in the colon sample stained positive for HNP 1–3. (D,E) Although small numbers of neutrophils in the blood vessels and submucosal tissues were positive for HNP 1–3, epithelial cells in colon samples from patients with inflamed CD or normal subjects were not positive for HNP 1–3. Original magnification: 100× (A,B) and 200× (C–E).

the level of HNP 1–3 had a high discriminatory power for estimating the efficacy of treatment in patients with UC.

DISCUSSION

We identified 27 proteins that showed significant differences in the serum protein profiles of patients with UC compared with those of healthy controls using SELDI-TOF/MS analysis. Of these proteins, 3 signals around 3400 m/z were confirmed to correspond to HNP 1, 2, and 3. In addition, we observed an increase in HNP 1–3 plasma levels in patients with active-phase UC compared with that seen in patients with remission-phase UC or CD; these levels were higher in the plasma of UC patients who showed better therapeutic outcomes than in samples from nonresponder patients.

Several studies have suggested that the development of IBD requires the interaction of genetic factors with both specific luminal bacterial antigens and environmental triggers that break the mucosal barrier.[16–18] Although the principle treatment for IBD is the suppression of inflammation, treatment strategies for the 2 diseases, UC and CD, are somewhat different. Whereas these differences may address the different biomarkers of the 2 conditions, a specific biomarker for IBD remains unknown. To discover a biomarker of UC, we

TABLE 3. Characteristics of Patients with Active UC in the Responder Group and Nonresponder Group

	Responder	Nonresponder	*P*-value
Number	8	7	
Gender (M/F)	5/3	5/2	0.7
Age (yr)	33.5 ± 13.8 [14–50]	42.3 ± 19.8 [16–68]	0.4
CRP (mg/dl)	1.7 ± 1.7	3.3 ± 4.5	0.4
WBC (cells/ul)	12714 ± 4604	7657 ± 3423	*0.04*
Platelets × 10^4/ul	40.4 ± 7.4	36.2 ± 11.1	0.3
HNP 1–3 (ng/ml)	273.0 ± 224.8	84.6 ± 26.5	*0.002*
Type of UC			
Pancolitis/Left-side colitis	7/1	5/2	0.6
UCDAI score	9.4 ± 4.6	8.6 ± 1.9	0.7
Duration	6.7 ± 6.5 [1–19]	5.7 ± 5.1 [2–16]	0.8

Data are shown as the means ± SD [ranges]. Statistical significance was determined using a Mann-Whitney *U*-test or Fisher's exact test, as appropriate. UC, ulcerative colitis; UCDAI, Ulcerative Colitis Disease Activity Index.

employed ProteinChip technology. The likelihood of finding reliable tumor markers by analyzing tissue may be higher than in analyses of serum[12]; malignant cells may produce proteins that are useful biomarkers. In nonmalignant diseases, such as UC, protein profiling of serum or plasma may be more informative than that of tissue samples. Additionally, fluid samples, such as serum, are easier to obtain than tissue samples. Thus, we used serum samples to identify new biomarkers for UC.

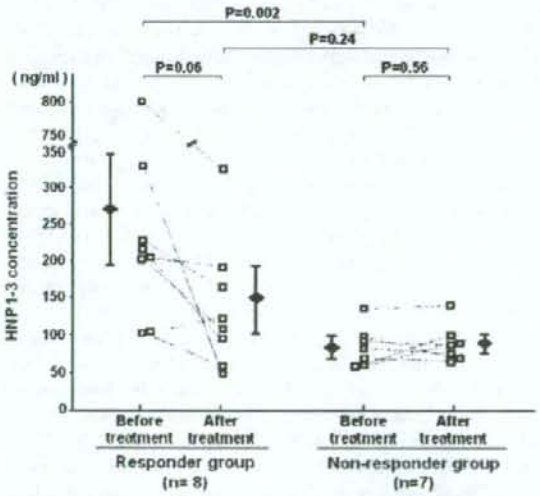

Figure 5. HNP 1–3 levels in the responder and nonresponder groups before treatment predicted therapeutic outcomes in UC patients; changes in the HNP 1–3 levels in UC patients in response to treatment are presented. The mean concentration of HNP 1–3 in the responder group before treatment was significantly higher than that seen in the nonresponder group, which indicates that HNP 1–3 levels may be an effective predictor of therapeutic outcomes. HNP 1–3 levels tended to decrease after treatment in the responder group, whereas no changes were observed for the nonresponder group. Patients whose plasma was not obtained after treatment were excluded from analysis.

Defensins are one of the most extensive peptide families of naturally occurring antibiotics. These peptides exhibit microbicidal activities against Gram-positive and Gram-negative bacteria, mycobacteria, fungi, and certain enveloped viruses. HNP 1–3 are part of the α-defensin family and components of the innate immune response. HNP 1–3 are synthesized by neutrophil precursor cells and released at inflammatory sites by mature circulating neutrophils.[9,19] The expression of HNP 1–3 has been observed in epithelial cells of the ileum and colon in patients with active UC or CD.[20] Whether neutrophils within inflamed colon tissue express HNP 1–3 in IBDs, however, is not known. In this study, we demonstrated that the colon mucosal tissue of patients with active UC or CD displayed minimal immunoreactivity for HNP 1–3, whereas the infiltrating neutrophils were stained strongly. These results indicate that HNP 1–3 were secreted from neutrophils, leading to increased plasma levels in patients with UC. High concentrations of HNP 1–3 can be cytotoxic for epithelial cells due to cytolysis and can induce apical conduction in Cl^- secretory epithelia.[21,22] Thus, whereas HNP 1–3 have antibacterial activities in the early phase of UC, they also may injure the colon if they are overexpressed by infiltrating neutrophils. High concentrations of HNP 1–3 may adversely affect colon tissues in UC patients, potentially contributing to diarrhea.[23] HNP 1–3 are secreted from the azurophilic granules of neutrophils following stimulation with IL-8.[24] Epithelial-derived IL-8 is thought to mediate neutrophil migration and infiltration during the inflammatory process of UC.[25,26] IL-8 mRNA levels are

significantly higher in UC patients with crypt abscesses.[27] Although HNP 1–3 have been reported to be expressed by surface enterocytes in the mucosa of patients with active IBD,[28] we observed only minimal staining of the colonic surface mucosa from patients with active UC using anti-HNP 1–3 antibodies. Moreover, Caco-2 and HT-29 cells, 2 colon epithelial cell lines, do not express HNP 1–3 (data not shown). Therefore, we hypothesized that HNP 1–3 are expressed by neutrophils following stimulation with IL-8, which suggested a correlation between the IL-8 and HNP 1–3 levels. We did not, however, observe a correlation between the IL-8 and HNP 1–3 levels in the plasma from active UC patients, and there was no association between the disease activity score and plasma IL-8 concentrations (data not shown). These results indicate that HNP 1–3 expression may be affected by other factors and HNP 1–3 values appear to be more useful to measure clinical UC disease activity than IL-8 levels.

Neutrophils are critical cellular mediators of the inflammation observed in UC. Neutrophils increase in number and display augmented activation during active-phase UC, but not inactive-phase UC.[28] Neutrophils extensively infiltrate colon tissue in patients with UC, and can be detected in the inflamed mucosa during even the early stages of inflammation.[29,30] Platelets are also important in the pathophysiology of UC.[31] Cytapheresis therapy (including LCAP) in combination with steroid therapy can be an effective treatment option for patients with active UC.[32] LCAP may remove and modulate both leukocytes and platelets, thereby altering the expression of proinflammatory cytokines.[33,34] The effect of LCAP on HNP 1–3 levels, however, has not been examined, and further studies are needed to determine whether HNP 1–3 levels decrease in response to LCAP. In addition, we showed that HNP 1–3 levels in the plasma were higher in patients with active UC than in those with infectious colitis, and HNP 1–3 levels were similar between patients with infectious colitis and healthy controls. In contrast, it was reported that HNP 1–3 levels in patients with severe infectious diseases, such as sepsis, were higher than those in healthy controls.[35] The disease severity of the enrolled patients with infectious colitis in this study may have affected our results. Cytapheresis therapy, however, may not be effective for severe infectious diseases, including infectious colitis, and high concentrations of HNP 1–3 in patients with active UC may be associated with disease characteristics. Further examination, including cases of infectious colitis with sepsis, will be necessary.

As previously reported, we found that several inflammatory makers, including the CRP level, WBC, and platelet count, decreased after treatment. Changes in these inflammatory markers did not predict the treatment outcome of patients with UC, whereas plasma levels of HNP 1–3 correlated with UC disease activity and predicted the therapeutic outcome. There were no correlations between plasma HNP 1–3 levels and inflammatory markers, such as platelet counts and CRP levels. These results may suggest that high levels of HNP 1–3 independently indicate the activity of disease and the feasible treatment outcome in patients with UC. However, there is a limitation in the use of HNP 1–3 measurement as a biomarker; low levels of HNP 1–3 in colitis patients did not diagnose whether they had nonresponder UC or active CD. Therefore, low levels of HNP 1–3 in colitis patients should be assessed by clinical symptoms, stool for bacterial examination, and endoscopic and radiographic examination of the gastrointestinal tract for diagnosis. Other proteins and peptides that were detected by SELDI/TOF-MS in this study are now under investigation and may serve as additional biomarkers for the assessment of IBD, especially in nonresponder UC patients.

The levels of HNP 1–3 in tumor tissue and serum were reported to increase in patients with CRC.[12] It was also reported that plasma HNP 1–3 concentrations determined using ELISA increased in Duke's stages C and D, but not in A or B compared to healthy controls.[14] In contrast, we showed that HNP 1–3 concentrations in CRC patients at Duke's stage A were higher than those seen in patients with inactive UC and healthy controls. Although HNP 1–3 concentrations in CRC patients at Duke's stage A seem to be similar between our study and a previous study[14] (100.8 ± 27.6 versus 105.4± 80.6 ng/mL, respectively), the concentrations in the healthy controls were different between the 2 studies (77.5 ±16.5 versus 96.6 ± 36.2 ng/mL). In addition, Albrethsen et al[14] mentioned that in addition to Duke's C and D, HNP 1–3 expression in CRC tissues at Duke's A and B was higher than in normal tissue by SELDI ProteinChip. It is controversial whether the increased HNP 1–3 in tumors is localized to cancer cells or to neutrophilic leukocytes. There is the possibility that the plasma HNP 1–3 levels will increase in patients with CRC at Duke's stage A and that HNP 1–3 concentration is a potential marker for the assessment of CRC patients with advanced disease.[12,14] In addition, these results indicate that HNP 1–3 levels may not be able to distinguish between active UC and colon cancer. In the clinical setting, however, UC can typically be distinguished from colon cancer by various clinical features, such as diarrhea, fever, and colonoscopic findings. On the other hand, colon cancer commonly occurs in patients with UC, especially those who have suffered from the disease for a long period of time; such colon cancers are difficult to detect using colonoscopy. HNP 1–3 levels may help to signal the occurrence of colon cancer in UC patients when high concentrations of HNP 1–3 are detected in the absence of active colitis; these patients should be extensively examined, including total colonoscopy and random biopsies.

In conclusion, we used SELDI-TOF/MS to perform serum protein profiling and determined that HNP 1–3 levels increase in patients with active-phase of UC. We also con-

firmed that HNP 1–3 are predictive markers for UC treatment outcomes. Although these markers may not distinguish UC from CRC, HNP 1–3 are useful markers for the differential diagnosis of patients with IBD.

ACKNOWLEDGMENT

We thank Ms. Yuko Nakamura and Ms. Yuka Takahama for technical assistance.

REFERENCES

1. Xavier RJ, Podolsky DK. Unravelling the pathogenesis of inflammatory bowel disease. *Nature*. 2007;448:427–434.
2. Podolsky DK. Inflammatory bowel disease. *N Engl J Med*. 2002;347:417–429.
3. Mazlam MZ, Hodgson HJ. Peripheral blood monocyte cytokine production and acute phase response in inflammatory bowel disease. *Gut*. 1992;33:773–778.
4. Vermeire S, Van Assche G, Rutgeerts P. Laboratory markers in IBD: useful, magic, or unnecessary toys? *Gut*. 2006;55:426–431.
5. Sutherland LR, Martin F, Greer S, et al. 5-Aminosalicylic acid enema in the treatment of distal ulcerative colitis, proctosigmoiditis, and proctitis. *Gastroenterology*. 1987;92:1894–1898.
6. Andre C, Descos L, Landais P, et al. Assessment of appropriate laboratory measurements to supplement the Crohn's disease activity index. *Gut*. 1981;22:571–574.
7. Kanmura S, Uto H, Kusumoto K, et al. Early diagnostic potential for hepatocellular carcinoma using the SELDI ProteinChip system. *Hepatology*. 2007;45:948–956.
8. de Seny D, Fillet M, Meuwis MA, et al. Discovery of new rheumatoid arthritis biomarkers using the surface-enhanced laser desorption/ionization time-of-flight mass spectrometry ProteinChip approach. *Arthritis Rheum*. 2005;52:3801–3812.
9. Ganz T, Selsted ME, Szklarek D, et al. Defensins. Natural peptide antibiotics of human neutrophils. *J Clin Invest*. 1985;76:1427–1435.
10. de Dombal FT, Softley A. IOIBD report no. 1: Observer variation in calculating indices of severity and activity in Crohn's disease. *Gut*. 1987;28:474–481.
11. Christian M, Günther E, Bettina S, et al. A technical triade for proteomic identification and characterization of cancer biomarkers. *Cancer Res*. 2004;64:4099–4104.
12. Melle C, Ernst G, Schimmel B, et al. Discovery and identification of alpha-defensins as low abundant, tumor-derived serum markers in colorectal cancer. *Gastroenterology*. 2005;129:66–73.
13. Adam BL, Qu Y, Davis JW, et al. Serum protein fingerprinting coupled with a pattern-matching algorithm distinguishes prostate cancer from benign prostate hyperplasia and healthy men. *Cancer Res*. 2002;62:3609–3614.
14. Albrethsen J, Moller CH, Olsen J, et al. Human neutrophil peptides 1, 2 and 3 are biochemical markers for metastatic colorectal cancer. *Eur J Cancer*. 2006;42:3057–3064.
15. Cunliffe RN. Alpha-defensins in the gastrointestinal tract. *Mol Immunol*. 2003;40:463–467.
16. Schmitz H, Barmeyer C, Fromm M, et al. Altered tight junction structure contributes to the impaired epithelial barrier function in ulcerative colitis. *Gastroenterology*. 1999;116:301–309.
17. Sugimura K, Asakura H, Mizuki N, et al. Analysis of genes within the HLA region affecting susceptibility to ulcerative colitis. *Hum Immunol*. 1993;36:112–118.
18. Kobayashi K, Atoh M, Konoeda Y, et al. HLA-DR, DQ and T cell antigen receptor constant beta genes in Japanese patients with ulcerative colitis. *Clin Exp Immunol*. 1990;80:400–403.
19. van Wetering S, Sterk PJ, Rabe KF, et al. Defensins: key players or bystanders in infection, injury, and repair in the lung? *J Allergy Clin Immunol*. 1999;104:1131–1138.
20. Cunliffe RN, Kamal M, Rose FR, et al. Expression of antimicrobial neutrophil defensins in epithelial cells of active inflammatory bowel disease mucosa. *J Clin Pathol*. 2002;55:298–304.
21. Sakamoto N, Mukae H, Fujii T, et al. Differential effects of alpha- and beta-defensin on cytokine production by cultured human bronchial epithelial cells. *Am J Physiol Lung Cell Mol Physiol*. 2005;288:508–513.
22. Merlin D, Yue G, Lencer WI, et al. Cryptdin-3 induces novel apical conductance(s) in Cl-secretory, including cystic fibrosis, epithelia. *Am J Physiol Cell Physiol*. 2001;280:296–302.
23. Fahlgren A, Hammarström S, Danielsson A, et al. Increased expression of antimicrobial peptides and lysozyme in colonic epithelial cells of patients with ulcerative colitis. *Clin Exp Immunol*. 2003;131:90–101.
24. Ashitani J, Mukae H, Nakazato M, et al. Elevated pleural fluid levels of defensins in patients with empyema. *Chest*. 1998;113:788–794.
25. Imada A, Ina K, Shimada M, et al. Coordinate upregulation of interleukin-8 and growth-related gene product-alpha is present in the colonic mucosa of inflammatory bowel. *Scand J Gastroenterol*. 2001;36:854–864.
26. McCormick BA, Hofman PM, Kim J, et al. Surface attachment of Salmonella typhimurium to intestinal epithelia imprints the subepithelial matrix with gradients chemotactic for neutrophils. *J Cell Biol*. 1995;131:1599–1608.
27. Bulois P, Tremaine WJ, Maunoury V, et al. Pouchitis is associated with mucosal imbalance between interleukin-8 and interleukin-10. *Inflamm Bowel Dis*. 2000;6:157–164.
28. Lampinen M, Rönnblom A, Amin K, et al. Eosinophil granulocytes are activated during the remission phase of ulcerative colitis. *Gut*. 2005;54:1714–1720.
29. Nikolaus S, Bauditz J, Gionchetti P, et al. Increased secretion of pro-inflammatory cytokines by circulating polymorphonuclear neutrophils and regulation by interleukin 10 during intestinal inflammation. *Gut*. 1998;42:470–476.
30. Kucharzik T, Walsh SV, Chen J, et al. Neutrophil transmigration in inflammatory bowel disease is associated with differential expression of epithelial intercellular junction proteins. *Am J Pathol*. 2001;159:2001–2009.
31. Andoh A, Yoshida T, Yagi Y, et al. Increased aggregation response of platelets in patients with inflammatory bowel disease. *J Gastroenterol*. 2006;41:47–54.
32. Sawada K, Muto T, Shimoyama T, et al. Multicenter randomized controlled trial for the treatment of ulcerative colitis with a leukocytapheresis column. *Curr Pharm Des*. 2003;9:307–321.
33. Sawada K, Ohnishi K, Fukui S, et al. Leukocytapheresis therapy, performed with leukocyte removal filter, for inflammatory bowel disease. *J Gastroenterol*. 1995;30:322–329.
34. Fukunaga K, Fukuda Y, Yokoyama Y, et al. Activated platelets as a possible early marker to predict clinical efficacy of leukocytapheresis in severe ulcerative colitis patients. *J Gastroenterol*. 2006;41:524–532.
35. Panyutich AV, Panyutich EA, Krapivin VA, et al. Plasma defensin concentrations are elevated in patients with septicemia or bacterial meningitis. *J Lab Clin Med*. 1993;122:202–207.

Exacerbating Role of γδ T Cells in Chronic Colitis of T-Cell Receptor α Mutant Mice

MASANOBU NANNO,* YASUYOSHI KANARI,‡ TOMOAKI NAITO,§,‖ NAGAMU INOUE,¶ TADAKAZU HISAMATSU,¶ HIROSHI CHINEN,¶ KEN SUGIMOTO,#,** YASUYO SHIMOMURA,#,** HIDEO YAMAGISHI,‡ TETSUO SHIOHARA,‡‡ SATOSHI UEHA,§§ KOUJI MATSUSHIMA,§§ MAKOTO SUEMATSU,‖ ATSUSHI MIZOGUCHI,#,** TOSHIFUMI HIBI,¶ ATUL K. BHAN,#,** and HIROMICHI ISHIKAWA§

*Yakult Central Institute for Microbiological Research, Tokyo; ‡Department of Biophysics, Graduate School of Science, Kyoto University, Kyoto; §Department of Microbiology and Immunology, Keio University School of Medicine, Tokyo; ‖Department of Biochemistry and Integrative Medical Biology, Keio University School of Medicine, Tokyo; ¶Department of Internal Medicine, Keio University School of Medicine, Tokyo, Japan; #Center for the Study of Inflammatory Bowel Disease, Massachusetts General Hospital, Boston; **Department of Pathology, Massachusetts General Hospital, Boston, Massachusetts; ‡‡Department of Dermatology, Kyorin University School of Medicine, Tokyo, Japan; and §§Department of Molecular Preventive Medicine, Graduate School of Medicine, University of Tokyo, Tokyo, Japan

Background & Aims: **T-cell receptor (TCR) γδ T cells are an important component of the mucosal immune system and regulate intestinal epithelial homeostasis. Interestingly, there is a significant increase in γδ T cells in the inflamed mucosa of patients with ulcerative colitis (UC). However, the role of γδ T cells in chronic colitis has not been fully identified.** ***Methods:*** **TCRα-deficient mice, which spontaneously develop chronic colitis with many features of human UC including an increase in γδ T-cell population, represent an excellent model to investigate the role of γδ T cells in UC-like colitis. To identify the role of γδ T cells in this colitis, we herein have generated TCRγ-deficient mice through deletion of all TCR Cγ genes (Cγ1, Cγ2, Cγ3, and Cγ4) using the *Cre/loxP* site-specific recombination system and subsequently crossing these mice with TCRα-deficient mice.** ***Results:*** **An increase in colonic γδ T cells was associated with the development of human UC as well as UC-like disease seen in TCRα-deficient mice. Interestingly, the newly established $TCR\alpha^{-/-} \times TCR\gamma^{-/-}$ double mutant mice developed significantly less severe colitis as compared with TCRα-deficient mice. The suppression of colitis in $TCR\alpha^{-/-} \times TCR\gamma^{-/-}$ double mutant mice was associated with a significant reduction of proinflammatory cytokine and chemokine productions and a decrease in neutrophil infiltration.** ***Conclusions:*** **γδ T cells are involved in the exacerbation of UC-like chronic disease. Therefore, γδ T cells may represent a promising therapeutic target for the treatment of human UC.**

T cell receptor (TCR) γδ T cells are an evolutionary conserved T-cell subset with characteristic properties.[1] TCRγδ-bearing murine dendritic epidermal T cells are involved in the regulation of epidermal integrity and promote wound repair of the skin,[2] whereas intestinal intraepithelial γδ T cells (γδ-IEL) regulate intestinal epithelial homeostasis.[3,4] Recent evidence suggests that γδ T cells are also important in immune surveillance of the epithelium by providing a first line of defense against infectious pathogens attacking the surfaces of the body and in the regulation of linking of innate and acquired immunity.[1,5] Furthermore, γδ T cells appear to down-regulate αβ T cell-driven robust immune responses that often result in severe immunopathology.[1]

The incidence of inflammatory bowel diseases (IBD), namely ulcerative colitis (UC) and Crohn's disease (CD), has increased markedly in recent years. The factors including genetic predisposition, environmental conditions, and aberrant immune response driven by normal intestinal flora are vital for the development and persistence of the inflammatory process.[6,7] In the present study, we aimed at elucidating the role of γδ T cells in the pathogenesis of IBD because there is growing evidence supporting that γδ T cells play an active multifaceted immunoregulatory role in the coordinated innate and acquired immune responses that maintain the integrity of epithelial tissues[1,2,4,5,8] and an increase in γδ T cells in the diseased mucosa has been documented in UC patients.[9,10] In acute colitis induced by administration of either 2,4,6-trinitrobenzene sulfonic acid[11,12] or dextran sulfate sodium,[13,14] a protective role of γδ T cells has been demonstrated. However, the role of γδ T cells in chronic intestinal inflammation resembling UC has not yet been investigated. $TCR\alpha^{-/-}$ ($\alpha^{-/-}$) mice spontaneously develop chronic colitis with several features of human UC including a significant increase in γδ T cells.[15] To illuminate the role of γδ T cells in the pathogenesis of UC-like colitis in $\alpha^{-/-}$ mice, we generated $TCR\gamma^{-/-}$

Abbreviations used in this paper: $\alpha^{-/-}$, $TCR\alpha^{-/-}$; ARP, anorectal prolapse; $\gamma^{-/-}$, $TCR\gamma^{-/-}$; γδ T cells, TCR γδ T cells; IBD, inflammatory bowel disease; IEL, intestinal intraepithelial T lymphocytes; LP, lamina propria; TCR, T-cell receptor; UC, ulcerative colitis.

0016-5085/08/$34.00
doi:10.1053/j.gastro.2007.11.056

($\gamma^{-/-}$) mice and examined the severity of colitis in $\alpha^{-/-}$ mice that are genetically engineered to lack γδ T cells.

Materials and Methods

Mice

We newly generated $\gamma^{-/-}$ mice and crossed with $\alpha^{-/-}$ mice[16] to develop double mutant ($\alpha^{-/-} \times \gamma^{-/-}$) mice. The generations of these mice are described in Supplementary Materials (see Supplemental Materials online at www.gastrojournal.org). All mice used were of C57BL/6 (B6) background. The mice were maintained under specific pathogen-free conditions, and all animal procedures described in this study were performed in accordance with the guidelines for animal experiments of Keio University School of Medicine, Yakult Central Institute for Microbiological Research, Kinki University School of Medicine, and Massachusetts General Hospital.

Flow Cytometry and Immunohistochemical Procedures

Methods for isolation of intestinal intraepithelial T cells (IEL) from mouse small intestines and lamina propria (LP) cells from mouse and human large intestines are described in Supplementary Materials. Procedures of cell staining for flow cytometric and immunohistochemical analyses are also described in Supplementary Materials (see Supplemental Materials online at www.gastrojournal.org).

Histologic Evaluation of Colitis

The disease score of colitis (0–10) was estimated in a blind fashion using previously described criteria, namely, a combination of both gross and histologic findings.[17] The gross score was rated as 0, presence of normal beaded appearance; 1, absence of beaded appearance of colon; 2, focally thickened colon; and 3, marked thickness of entire colon. The histologic score was based on the extent of intestinal wall thickening (0–3), inflammatory cell infiltration into LP (0–3), and presence (0 or 1) of ulceration.

Real-Time Reverse-Transcription Polymerase Chain Reaction Analysis

Total RNA was extracted from half of the frozen colonic tissue obtained from each one of wild-type (WT), $\gamma^{-/-}$, $\alpha^{-/-}$, and $\alpha\gamma^{-/-}$ littermate mice, and complementary DNA (cDNA) was prepared. Quantitative real-time reverse-transcription polymerase chain reaction (RT-PCR) was conducted to assess the expression level of TNF-α, IL-1β, IL-6, TGF-β, IFN-γ, IL-7, IL-10, IL-12, KC, MIP-2, GCP-2, MCP-1, MIP-1α, MIP-1β, and HPRT genes using TaqMan probes (Applied Biosystems, Foster City, CA). The relative expression level of genes of interest was normalized to the HPRT gene expression. The detailed procedures are described in Supplementary Materials (see Supplemental Materials online at www.gastrojournal.org).

Measurement of Cytokines and Chemokines by Enzyme-Linked Immunosorbent Assay

Proteins were extracted from the above-described half of the frozen colonic tissue obtained from each one of WT, $\gamma^{-/-}$, $\alpha^{-/-}$, and $\alpha\gamma^{-/-}$ littermate mice. In brief, frozen colonic tissue was homogenized with a sonicator (Ultrasonic Disruptor UD-201, TOMY, Tokyo, Japan) in 5 mL lysis buffer (50 mmol/L Tris-HCl, pH 7.4, 150 mmol/L NaCl, 1% NP-40, 1 mmol/L dithiothreitol, 1 mmol/L EDTA, 1 mmol/L NaF, 1 mmol/L sodium orthovanadate, and complete, Mini EDTA-free proteinase inhibitor [Roche Applied Science, Mannheim, Germany]), the homogenate was clarified by centrifugation at 14,000 rpm for 10 minutes, and the supernatant was subjected to OptEIA ELISA (BD Biosciences, San Diego, CA) for detection of tumor necrosis factor (TNF)-α, interleukin (IL)-1β, and IL-6 and to DuoSet ELISA (R&D Systems, Minneapolis, MN) for detection of transforming growth factor (TGF)-β, interferon (IFN)-γ, keratinocyte-derived chemokine (KC), macrophage inflammatory protein (MIP)-2 and granulocyte chemotactic protein (GCP)-2. Levels in the supernatants were standardized to the total amount of protein in the same supernatants assessed by RC DC Protein Assay (Bio-Rad Laboratories, Hercules, CA).

Chemotaxis Assay

The assays were performed using the ChemoTx 96-well plate No. 101-3 (NeuroProbe, Gaithersburg, MD). Briefly, bone marrow cells collected from femurs, tibias, and humerus of WT mice were recovered by centrifugation at the interphase of 44% and 70% Percoll solutions. Subsequently, 2.5×10^5 bone marrow cells were loaded onto the membrane plate and placed on a flat-bottomed, 96-well microtiter plate containing the colon extracts (0.7 mg protein/mL) from WT, $\alpha^{-/-}$, and $\alpha\gamma^{-/-}$ mice in addition to serially diluted MIP-2 and MCP-1 (R&D Systems). To identify the neutrophils and monocytes, bone marrow cells were labeled with fluorescent dye conjugated monoclonal antibodies (mAb) to Mac-1 and Ly-6C before the assay. After incubation at 37°C for 2 hours, the number of Mac-1$^+$Ly-6C^{low} neutrophils[18] and Mac-1$^+$Ly-6C^{high} monocytes[18] that migrated into the lower wells was determined by a flow cytometry.

Cell Transfer

γδ T cells were purified from the mesenteric lymph nodes (MLNs) and colon of $\alpha^{-/-}$ mice through MACS system, and 2×10^6 purified cells were intravenously transferred twice into $\alpha\gamma^{-/-}$ mice (n = 16) at 4 and 5 months of age. As control group, phosphate-buffered saline (PBS) was intravenously administrated into $\alpha\gamma^{-/-}$ mice (n = 15). The recipient mice were then killed at 6 months of age.

Statistical Analysis

The statistical difference was determined by 2-sided Student *t* test. For the statistical analysis of cell infiltration into the large intestine, 2-sided Mann–Whitney *U* test was used. Difference with $P < .05$ was considered significant.

Results

Generation of TCRγ-Deficient Mice

To begin with, we initially confirmed that γδ T cells were increased in the lymphoid cells isolated from the inflamed colonic mucosa of UC patients as compared with those from the unaffected colonic mucosa of patients with colon cancer (Figure 1*A* and *B*) and also in the lymphoid cells isolated from the inflamed colonic LP of $\alpha^{-/-}$ mice as compared with those from normal colonic LP of age-matched WT littermate mice (Figure 1*C* and *D*).

Precise appreciation of the role of γδ T cells in pathogenesis of colitis in $\alpha^{-/-}$ mice requires the generation of $\alpha^{-/-}$ mice deficient in γδ T cells. However, the previously generated TCR$\delta^{-/-}$ ($\delta^{-/-}$) mice[19] lacking γδ T cells could not be used for this purpose because of the genomic localization of TCRδ coding segments within the *V* and *J* segments of TCRα gene.[20] To overcome this difficulty, we newly generated TCR$\gamma^{-/-}$ mice by disrupting the genes encoding TCR Cγ1, 2, 3, and 4 (CγΔ) using the Cre/*loxP* site-specific recombination system shown in Figure 2. The targeting vector pCγ4ΔNL carrying a *loxP*-flanked *pgk-neo* gene cassette in place of exon 1 of the Cγ4 gene (Figure 2*A*) was introduced into the embryonic stem (ES) clone Vγ6ΔL carrying the allele in which the Vγ6 region was replaced by a single *loxP* site (Figure 2*B*). Transfected cells were cultured in the presence of G418, and G418-resistant recombinant clones showing the joint transmission of Vγ6ΔL and Cγ4ΔNL genes were selected. These ES clones, including the clones carrying both transgenes on the same chromosome, Vγ6ΔL-Cγ4ΔNL (Figure 2*C*), were injected into B6 blastocysts. The chimeric mice obtained were crossed to the CAG-*cre* transgenic B6 mice to generate the Cγ1-, 2-, 3-, and 4-depleted TCRγ-deficient (CγΔ) allele (Figure 2*C*) by *cre*-mediated recombination in F_1 mice during embryonic development.

Subsequently, these F_1 mice were intercrossed to produce homozygous ($\gamma^{-/-}$) mice (Figure 2*D*), and these mutant $\gamma^{-/-}$ mice were backcrossed 8 times to B6 mice to obtain $\gamma^{-/-}$ mice carrying the B6 background. WT ($\alpha^{+/-} \times \gamma^{+/-}$), $\gamma^{-/-}$ ($\alpha^{+/-} \times \gamma^{-/-}$), $\alpha^{-/-}$ ($\alpha^{-/-} \times \gamma^{+/-}$), and $\alpha\gamma^{-/-}$ ($\alpha^{-/-} \times \gamma^{-/-}$) littermate F_2 mice were then produced by intercrossing $\alpha^{-/-}$ mice[16] with $\gamma^{-/-}$ mice. Flow cytometric analysis of IEL from the small intestine confirmed that γδ T cells were absent in $\gamma^{-/-}$ and $\alpha\gamma^{-/-}$ mice (Figure 2*E*).

Pathogenic Role of γδ T Cells in UC-Like Colitis

Histologic examination of the colons from 20- to 32-week-old $\alpha^{-/-}$ and $\alpha\gamma^{-/-}$ mice revealed that inflam-

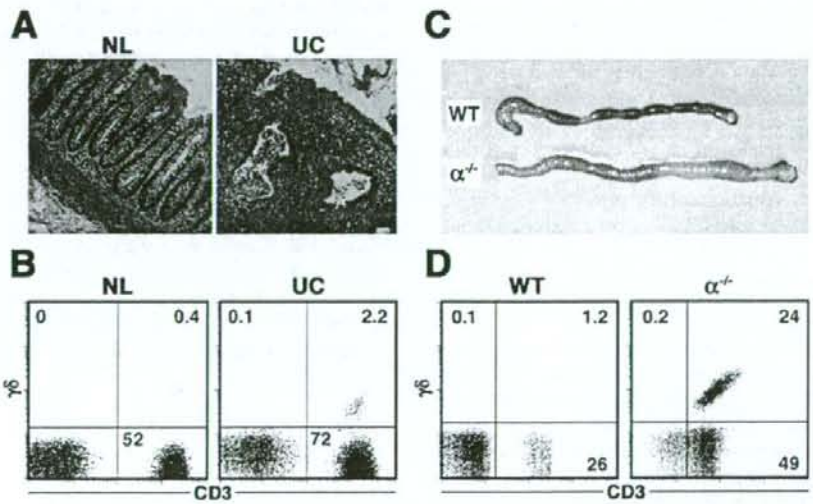

Figure 1. γδ T cells concentrate in the inflamed colonic mucosa of UC patients and colonic LP of $\alpha^{-/-}$ mice suffering from spontaneous chronic colitis. (*A*) A representative colonic tissue section from an ulcerative colitis (*UC*) patient shows a marked infiltration of lymphomyeloid cells, mucosal distortion, crypt abscess, and depletion of goblet cells compared with a normal colonic tissue section (*NL*) (original magnification, ×100). (*B*) A flow cytometry shows increased γδ T-cell population in a diseased colonic LP of UC patient compared with that in a normal colonic LP. This is a representative result of 3 UC patients. (*C*) Large intestines from wild-type (*WT*) mice and $\alpha^{-/-}$ mice suffering from spontaneous chronic colitis are shown. (*D*) A flow cytometry shows increased γδ T-cell population in a diseased colonic LP of $\alpha^{-/-}$ mice compared with that in colonic LP of WT littermate.

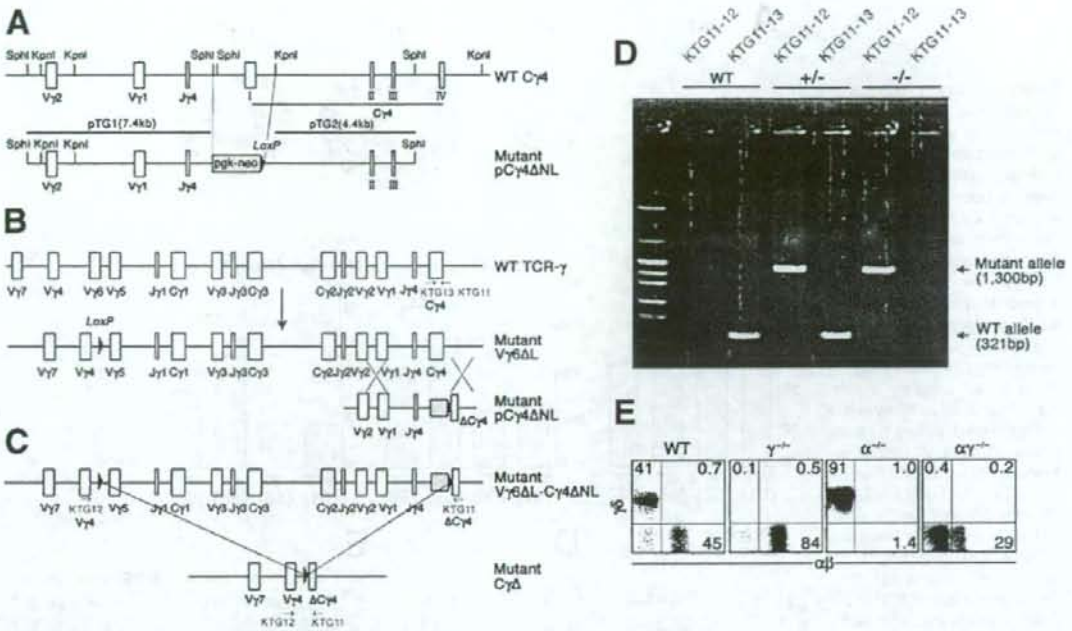

Figure 2. Generation of TCRγ-deficient mice and subsequent production of TCRαγ double mutant mice. (*A*) Schematic representation of WT and mutant (pCγ4ΔNL) genomic Cγ4 loci together with the 3 DNA fragments used to construct the mutant pCγ4ΔNL vector. The resulting targeting vector (pCγ4ΔNL) carrying a *loxP*-flanked *pgk-neo* gene cassette in place of exon 1 of Cγ4 gene used a neomycin resistance gene driven by the *pgk* promoter as positive selection marker is shown. Restriction enzyme sites, *SphI* and *KpnI* (*solid bars*), exon structures, Vγ and Jγ (*open boxes*), and *loxP* site (*solid triangle*) are indicated. (*B*) Schematic representation of the ES clone carrying WT TCRγ gene and mutant Vγ6ΔL ES clone carrying the allele in which the Vγ6 region was replaced by a single *loxP* site and mutant pCγ4ΔNL targeting vector. Exon structures, Vγ and Jγ (*open boxes*) and *loxP* site (*solid triangle*) are indicated. (*C*) Schematic representation of generation of the mutant mice that carry the TCRγ-deficient (CγΔ) allele by Cre-mediated recombination during embryonic development. Exon structures, Vγ and Jγ (*open boxes*), and *loxP* site (*solid triangle*) are indicated. (*D*) The mutant mice that carry the TCRγ-deficient (CγΔ) allele were intercrossed to produce TCRγ$^{-/-}$ (WT), TCRγ$^{+/-}$ (γ$^{+/-}$), and TCRγ$^{-/-}$ (γ$^{-/-}$) mice, and the corresponding WT and mutant alleles were typed by PCR analysis of tail DNA with each set of primers indicated. (*E*) γδ T cells are absent from the IEL compartment of γ$^{-/-}$ and αγ$^{-/-}$ mice. γ$^{-/-}$ Mice were crossed with α$^{-/-}$ mice to obtain WT (α$^{+/-}$ × γ$^{+/-}$), γ$^{-/-}$ (α$^{+/-}$ × γ$^{-/-}$), α$^{-/-}$ (α$^{-/-}$ × γ$^{+/-}$), and αγ$^{-/-}$ (α$^{-/-}$ × γ$^{-/-}$) littermate mice.

mation characterized by elongation of crypts was much milder in αγ$^{-/-}$ mice as compared with α$^{-/-}$ mice (Figure 3*A*). Although the body weight was comparable between αγ$^{-/-}$ and α$^{-/-}$ mice, it was evident that colonic weight was significantly decreased in αγ$^{-/-}$ mice as compared with α$^{-/-}$ mice (Figure 3*B*). The disease score characterized by the thickening of colonic mucosa with crypt elongation and inflammatory cell infiltration was also significantly lower in αγ$^{-/-}$ mice than that rated in α$^{-/-}$ mice (Figure 3*C*). Although approximately 20% of 20- to 60-week-old α$^{-/-}$ mice displayed anorectal prolapse (ARP), it was not discerned in any of age-matched αγ$^{-/-}$ mice (Figure 3*D*). Notably, no difference was observed in the age of onset of colitis and in the incidence of colitis (~80%) among 20- to 32-week-old αγ$^{-/-}$ and α$^{-/-}$ mice. In addition, in comparison with administration of PBS (as control), adoptive transfer of γδ T cells that were purified from α$^{-/-}$ mice did not increase the incidence of colitis in the recipient αγ$^{-/-}$ mice. However, the transfer of γδ T cells exacerbated the severity of colitis in the recipient αγ$^{-/-}$ mice. As shown in Figure 3*E*, more severe inflammatory cell infiltration was observed in the inflamed colon of the recipient αγ$^{-/-}$ mice with γδ T-cell transfer as compared with control αγ$^{-/-}$ mice. Therefore, it is possible that γδ T cells may be involved in the exacerbation, but not induction, of UC-like colitis.

Decrease in the Colonic Neutrophils and Monocytes in the Absence of γδ T Cells

The above results indicate that the spontaneous colitis in α$^{-/-}$ mice is ameliorated by the absence of γδ T cells in αγ$^{-/-}$ mice. With these findings in mind, flow cytometric analysis of colonic LP cells isolated from WT, γ$^{-/-}$, α$^{-/-}$, and αγ$^{-/-}$ littermate mice at approximately 28 weeks of age was performed, and the representative results of 5 independent experiments are presented in Figure 4*A*. In this experiment, WT, γ$^{-/-}$, α$^{-/-}$, and αγ$^{-/-}$ littermate mice yielded 5.1 × 10^5, 6.1